



UNIVERSITY OF HELSINKI

<https://helda.helsinki.fi>

Vertical profiles of volatile organic compounds and fine particles in atmospheric air by using an aerial drone with miniaturized samplers and portable devices

Pusfitasari, Eka Dian; Ruiz-Jimenez, Jose; Tiisanen, Aleks; Suuronen, Markus; Haataja, Jesse Juhani ...

2023-05-30

Copernicus GMBH

<http://hdl.handle.net/10138/358313>

Pusfitasari, E D, Ruiz-Jimenez, J, Tiisanen, A, Suuronen, M, Haataja, J J, Wu, Y, Kangasluoma, J, Luoma, K, Petäjä, T, Jussila, M, Hartonen, K & Riekkola, M-L 2023, 'Vertical profiles of volatile organic compounds and fine particles in atmospheric air by using an aerial drone with miniaturized samplers and portable devices', *Atmospheric Chemistry and Physics*, vol. 23, no. 10, pp. 5885-5904. <https://doi.org/10.5194/acp-23-5885-2023>

Downloaded from Helda, University of Helsinki institutional repository. <https://helda.helsinki.fi>
This is an electronic reprint of the original article.
This reprint may differ from the original in pagination and typographic detail.
Please cite the original version.



Vertical profiles of volatile organic compounds and fine particles in atmospheric air by using an aerial drone with miniaturized samplers and portable devices

Eka Dian Pusfitasari^{1,2}, Jose Ruiz-Jimenez^{1,2}, Aleksii Tiusanen¹, Markus Suuronen¹, Jesse Haataja³, Yusheng Wu³, Juha Kangasluoma³, Krista Luoma^{3,4}, Tuukka Petäjä³, Matti Jussila^{1,2}, Kari Hartonen^{1,2}, and Marja-Liisa Riekkola^{1,2}

¹Department of Chemistry, P.O. Box 55, 00014 University of Helsinki, Helsinki, Finland

²Institute for Atmospheric and Earth System Research, Chemistry, Faculty of science, P.O. Box 55, 00014 University of Helsinki, Helsinki, Finland

³Institute for Atmospheric and Earth System Research, Physics, Faculty of science, P.O. Box 64, 00014 University of Helsinki, Helsinki, Finland

⁴Finnish Meteorological Institute, P.O. Box 503, 00101 Helsinki, Finland

Correspondence: Kari Hartonen (kari.hartonen@helsinki.fi) and Marja-Liisa Riekkola (marja-liisa.riekkola@helsinki.fi)

Received: 26 January 2023 – Discussion started: 27 January 2023

Revised: 6 April 2023 – Accepted: 22 April 2023 – Published: 30 May 2023

Abstract. The increase in volatile organic compound (VOC) emissions released into the atmosphere is one of the main threats to human health and climate. VOCs can adversely affect human life through their contribution to air pollution directly and indirectly by reacting via several mechanisms in the air to form secondary organic aerosols. In this study, an aerial drone equipped with miniaturized air-sampling systems including up to four solid-phase microextraction (SPME) Arrows and four in-tube extraction (ITEX) samplers for the collection of VOCs, along with portable devices for the real-time measurement of black carbon (BC) and total particle numbers at high altitudes was exploited. In total, 135 air samples were collected under optimal sampling conditions from 4 to 14 October 2021 at the boreal forest SMEAR II station, Finland. A total of 48 different VOCs, including nitrogen-containing compounds, alcohols, aldehydes, ketones, organic acids, and hydrocarbons, were detected at different altitudes from 50 to 400 m above ground level with concentrations of up to 6898 ng m⁻³ in the gas phase and 8613 ng m⁻³ in the particle phase. Clear differences in VOC distributions were seen in samples collected from different altitudes, depending on the VOC sources. It was also possible to collect aerosol particles by the filter accessory attached on the ITEX sampling system, and five dicarboxylic acids were quantified with concentrations of 0.43 to 10.9 μg m⁻³. BC and total particle number measurements provided similar diurnal patterns, indicating their correlation. For spatial distribution, BC concentrations were increased at higher altitudes, being 2278 ng m⁻³ at 100 m and 3909 ng m⁻³ at 400 m. The measurements aboard the drone provided insights into horizontal and vertical variability in BC and aerosol number concentrations above the boreal forest.

1 Introduction

The global phenomenon of climate change has attracted huge attention in the past decades. Atmospheric aerosol particles can influence the climate system directly by scattering sunlight, transmission, and absorption of radiation and indirectly by acting as nuclei for cloud formation (Hemmilä, 2020; Kim et al., 2017; Oh et al., 2020). Fine aerosol particles have sizes close to the wavelength range of visible light; therefore, they are expected to have a stronger climatic impact than larger particles (Kanakidou et al., 2005). In addition, aerosol particles also have an adverse effect on air quality and human health by exposing a human's respiratory system to aerosol particulate matter (PM) that can get into lungs and translocate into vital organs due to their tiny size (Fu et al., 2013).

The formation and growth process of aerosol particles have been studied by many research groups (Ahlberg et al., 2017; Camredon et al., 2007; Casquero-Vera et al., 2020; Kulmala et al., 2013, 2014; Peng et al., 2021; Ziemann and Atkinson, 2012). To study particle formation in the atmosphere, it is important to assess the possible sources of the atmospheric particles, e.g., by the presence of volatile organic compounds (VOCs). Hydrocarbons and amines, for example, have been extensively investigated by modeling or by laboratory chamber experiments to show their contribution to secondary organic aerosol (SOA) formation. These VOCs, along with other thousands of organic gaseous trace species, are directly emitted from biogenic and anthropogenic sources. In the atmosphere, VOCs are oxidized by reactions with atmospheric oxidants such as O_3^- , OH^- , NO_3^- , and Cl^- radicals to form less-volatile products and subsequently partition into aerosol particles, leading to SOA formation (Almeida et al., 2013; Kulmala et al., 2014; Zahardis et al., 2008; Ziemann and Atkinson, 2012). The SOAs then become the major components of fine aerosol particulate matter, such as PM_{10} and $\text{PM}_{2.5}$, which pollutes the environment (Fermo et al., 2021; Ge et al., 2011; Kulmala et al., 2014).

Another important component that contributes to air pollution is black carbon (BC), which is emitted mostly as a byproduct of fossil fuel combustion and biomass burning (Hyvärinen et al., 2011). In addition, industry, energy production, and domestic cooking contribute to BC in the atmosphere (Kumar et al., 2015). BC has been associated with adverse effects on human health, such as premature mortality, as well as on earth temperature and climate, since it absorbs solar radiation very strongly (Anenberg et al., 2012; Jacobson, 2010).

In addition to VOCs and BC, atmospheric organic acids, such as low-molecular-weight (LMW) dicarboxylic acids, are also recognized as ubiquitous aerosol constituents in the urban region. As highly water-soluble compounds, they have the capability to significantly enhance the hygroscopicity of aerosol particles (Kanakidou et al., 2005). LMW diacids can be emitted from biomass burning, vehicular exhausts, and natural marine ecosystems. They can also be produced from

the atmospheric photo-oxidation of various organic precursors (Fu et al., 2013; Kawamura and Sakaguchi, 1999; Rinaldi et al., 2011).

Condensation particle counters (CPCs) are important devices for the measurement of aerosol number concentrations and aerosol particle fluxes (McMurry, 2000; Kangasluoma and Attoui, 2019; Petäjä et al., 2001). CPCs are commonly used in ambient air quality monitoring to measure the number concentration of airborne submicron particles with sizes down to a few nanometers (Asbach et al., 2017; Buzorius et al., 1998). Conventional CPCs have generally not been used as portable devices due to their weight and size. However, recently, small CPCs are emerging and are being deployed, for example, for vertical profiling aboard drones (Kim et al., 2018; Carnerero et al., 2018) and other platforms (Petäjä et al., 2012).

In our previous research, we used reliable and versatile miniaturized air-sampling (MAS) techniques, which have many benefits for on-site sampling, such as small size, low sampling time, environmental friendliness, easy operation, and flexibility for practical applications and automation (Lan et al., 2020; Pusfitasari et al., 2022; Ruiz-Jimenez et al., 2019). Solid-phase microextraction (SPME) Arrow and in-tube extraction (ITEX) sampling systems have been successfully employed for the reliable collection of VOCs from ambient air samples (Lan et al., 2019a, b; Pusfitasari et al., 2022). An exhaustive sampling technique, the ITEX sampling system, with large sorbent volume can be fully automated, and it provides continuous air sampling, reliable analysis, and quantification (Lan et al., 2019a; Pusfitasari et al., 2022). As an active sampler, the ITEX system allows for the simultaneous collection of gas- and particle-phase compounds. Extra sampling accessories, including adsorbent trap and filter accessories together with ITEX, have enhanced the selectivity of the sampling system and allowed the ITEX system to collect only the gas phase (Pusfitasari et al., 2022). After sample collection, the compounds were desorbed from the samplers, separated, and detected by thermal desorption (TD) gas chromatography–mass spectrometry (GC-MS).

In this study, the sampling of VOCs and measurement of total particle number concentration and black carbon (BC) directly at various altitudes, from 50 to 400 m, were performed using an aerial drone as the platform as in our previous research (Lan et al., 2021; Pusfitasari et al., 2022; Ruiz-Jimenez et al., 2019). The sampling platform contained now up to four SPME Arrows and four ITEX units, with an additional portable commercial BC device for BC real-time measurement and a lab-made portable CPC for total particle number observation. The compositions of different gas-phase fractions collected by both the SPME Arrow and ITEX systems, aerosol particles collected by the ITEX sampling system including filter accessory, and BC and particle numbers were evaluated at different altitudes and temporal variations at the boreal forest SMEAR II station in October 2021. In ad-

dition, the possible correlation between VOCs, BC, and total particle number concentrations was also clarified.

2 Materials and methods

2.1 Reagent and materials

Detailed information of reagents used, including their purities, is given in the Supplement S1.

Empty ITEX units, divinylbenzene-polydimethylsiloxane (DVB-PDMS), and carbon-coated WR-SPME Arrow systems were purchased from BGB Analytik AG (Zurich, Switzerland). TENAX-GR was purchased from Altech (Deerfield, IL, USA). The mesoporous silica-based materials, the Mobil Composition of Matter No. 41 (MCM-41), and titanium hydrogen phosphate-modified (MCM-41-TP) materials were synthesized via solgel template as described in our previous publication (Lan et al., 2019b). The instructions for ITEX packing with 30 mg MCM-41-TP and 60 mg TENAX-GR are described in Lan et al. (2019a). The preparation of MCM-41-SPME Arrow with the sorbent thickness of 40 μm and length of 20 mm is found in Lan et al. (2019b).

2.2 Instrumentation

A lab-made permeation system was employed to create an artificial gas-phase sample in the laboratory (Lan et al., 2019a, 2021; Pusfitasari et al., 2022). A PAL Cycle Composer and PAL RTC autosampler that were used for sample collection and desorption in the laboratory were from CTC Analytics (Zwingen, Switzerland). An Agilent 6890N gas chromatograph coupled with an Agilent 5975C mass spectrometer (Agilent Technologies, Pittsburg, PA, USA) was used for the method optimization and quality assurance tests for air samples in the laboratory. For on-site analysis, an Agilent 6890 N gas chromatograph (Agilent Technologies, Pittsburg, PA, USA) equipped with a lab-made ITEX heater for thermal desorption was employed and coupled to an Agilent 5973 mass spectrometer. The GC capillary column used for the chromatographic separations was an InertCapTM for amines (30 m length \times 0.25 mm i.d., without any information for the film thickness, GL Sciences, Tokyo, Japan).

For organic acid determination, an Agilent 1260 Infinity high-performance liquid chromatography (HPLC) system equipped with a binary pump, autosampler, degassing unit, and a column compartment were employed and coupled to an Agilent 6420 triple-quadrupole mass spectrometer with electrospray ion source (ESI) (Agilent Technologies, Palo Alto, CA, USA). Chromatographic separations were performed with a 2.1 \times 150 mm SeQuant[®]ZIC[®]-cHILIC (3 μm particle size) hydrophilic interaction liquid chromatography (HILIC) column (Merck KGaA, Darmstadt, Germany). A KrudKatcher ULTRA HPLC in-line filter (0.5 μm) from Phenomenex Inc (Torrance, CA, USA) protected the column from particulate impurities.

2.3 Drone platform construction

A remote-controlled Geodrone X4L (Videodrone, Finland), similar to that used in our previous studies (Lan et al., 2021; Pusfitasari et al., 2022) with some modifications, was employed to carry out miniaturized air sampling and analyses (Fig. 1). With the dimension of 58 \times 58 \times 37 cm (width \times depth \times height), it could carry the modified sampling box including our MAS system (up to four SPME Arrow units and up to four ITEXs) with a new, light sampling pump for the ITEX system. In addition, some portable devices were also attached to the drone to measure black carbon (BC) and particle sizes by condensation particle counter (CPC). The BC portable device in the field was an AethLabs AE51-S6-1408, with an application version of 2.2.4.0 (San Francisco, CA, USA). It was operated at 880 nm wavelength, with an airflow rate of 99 mL min⁻¹. The portable CPC was laboratory made. The portable CPC measured total aerosol particle number concentration between sizes from 20 nm and 5 μm . The references for BC and particle concentrations were measured at the boreal forest SMEAR II station at an altitude of 4 m by an AE33 (operated at 880 nm) and an aerosol electrometer (TSI 3772), respectively.

2.4 Gas chromatography–mass spectrometry analysis

The SPME Arrow and ITEX sampling systems were preconditioned at 250 $^{\circ}\text{C}$ for 10 min under inert N₂ gas. Prior to sampling, decafluorobiphenyl vapor (as an internal standard) was spiked to SPME Arrow and ITEX for 1 min and 5 mL, respectively. After sampling, the SPME Arrow unit was injected to the GC inlet to desorb the analytes at a temperature of 250 $^{\circ}\text{C}$ for 1 min, while for ITEX, 800 μL of He was aspirated to the ITEX syringe, and the analytes were desorbed at a temperature of 250 $^{\circ}\text{C}$ and injected into the GC-MS system by moving the plunger down with the injection speed of 200 $\mu\text{L s}^{-1}$. All the analyses were done in splitless injection at 250 $^{\circ}\text{C}$. For chromatographic separations, the GC oven temperature was programmed from 40 $^{\circ}\text{C}$ (held for 2 min) to 250 $^{\circ}\text{C}$ (held for 10 min) at a rate of 20 $^{\circ}\text{C min}^{-1}$. The temperature of transfer line, ion source, and quadrupole were 250, 230, and 150 $^{\circ}\text{C}$, respectively. Electron ionization (EI) mode (70 eV) was used, and the scan range was from m/z 15 to 350. Helium (99.996 %, AGA, Espoo, Finland) was used as a carrier gas at a constant flow rate of 1.2 mL min⁻¹.

2.5 Hydrophilic interaction liquid chromatography–tandem mass spectrometry method for organic acid analysis

Acetonitrile (ACN) was used as the main organic solvent containing 0.01 % of formic acid (FA) (as Eluent A), while Eluent B was aqueous 0.01 % FA solution. The applied liquid chromatography (LC) gradient was the following: 5 % B (0–6 min), 5 % to 20 % B (5–18 min), and post run for 15 min.

The flow rate for the analysis was 0.25 mL min^{-1} , and column temperature was maintained at 40°C . The injection volume was $10 \mu\text{L}$. The LC system was coupled to the triple quadrupole mass spectrometer equipped with ESI. The ion source was operated in both positive and negative modes.

2.6 Method development, quality control, and quality assurance studies

The optimization study for the MCM-41-TP-ITEX system, including optimization of the adsorption and desorption processes, sampling kinetics, breakthrough volume, and the recovery of the storage time, has been carried out in our previous study using multivariate analysis (Pusfitasari et al., 2022). The evaluation and validation of SPME Arrow units coated with MCM-41, DVB-PDMS, and carbon wide range (Carbon WR) for the sampling of VOCs have also been studied in our previous research (Helin et al., 2015; Lan et al., 2019b).

For the TENAX-GR-ITEX sampler, the same method development and validation including the determination of optimum flow rate, repeatability, reproducibility, and sample storage were done by using our laboratory-made autosampler. The repeatability and reproducibility of the TENAX-GR-ITEX system were studied by analyzing the model compounds with five different ITEX units five times each. The sampling flow rate (47 mL min^{-1}) was measured at least once for each ITEX during the comparison.

The storage study was performed by keeping the TENAX-GR-ITEX system at room temperature and in a freezer (-20°C). The purpose was to monitor how conditions affect the adsorption of chemicals in the surrounding environment to TENAX-GR during storage. The retainment of adsorbed analytes in different conditions was also monitored. The difference in recovery between control sample (not stored) and stored sample was regarded as the loss of the compound.

2.7 Application, measurement sites, and sample collection in the field

The field sampling was carried out at the SMEAR II station (Station for Measuring Ecosystem–Atmosphere Relations; Hari and Kulmala, 2005; with the coordinates of 61.84263°N , 24.29013°E), Hyytiälä, from 4 to 14 October 2021. As many as 53 drone flights were performed, and 135 air samples in total were collected (67 samples were collected using ITEX and 68 using SPME Arrow sampling systems). Table 1 shows the summary of sampling and measurement techniques used in this study.

SPME Arrow units with different coating materials, DVB/PDMS, MCM-41, Carbon WR, were exploited to collect gas-phase samples. MCM-41-TP-ITEX and TENAX-GR-ITEX sampling systems were used to simultaneously collect the gas phase and particles. In the field study, the measured ITEX airflow ranged from 40 to 78 mL min^{-1} . The

flow was carefully measured before the sampling and after analyte desorption. ITEX sampling volumes were then obtained by multiplying the value of ITEX airflow rate with the sampling time. Other sampling variables, such as sampling location, remained constant.

To study the average composition of VOCs in the atmosphere (Sect. 3.3), the samples were collected simultaneously by ITEX and SPME Arrow systems located on the drone at altitudes from 50 to 400 m. Composition samples were collected for 2 min at each altitude and during the descending of the drone by starting at the highest altitude of 400 m, followed by 300, 200, 100, and 50 m (Supplement Fig. S1). In this case, the total sampling time was 13–14 min (consisting of a total of 10 min at different altitudes and 3–4 min when the drone was descending from 400 to 50 m), with a total flight time close to 20 min including takeoff and landing.

The VOC composition at altitudes of 50 and 400 m was also separately determined (Sect. 3.6). A detailed schematic picture of our sampling system is seen in Supplement Fig. S2 (sampling at 50 m for 10 min) and Supplement Fig. S3 (sampling at 400 m for 10 min).

Evaluation of ITEX sampling with the filter accessory was also studied (Sect. 3.4). TENAX-GR-ITEX furnished with the filter accessory was employed to collect the gas phase only. A polytetrafluoroethylene (PTFE) filter with a pore size of $0.2 \mu\text{m}$ (diameter of 13 mm, VWR) was used as the ITEX filter accessory to remove aerosol particles from the natural air samples. The results obtained were directly compared with those achieved by the Carbon WR-SPME Arrow sampling system. The recovery was calculated from the difference between concentrations obtained by SPME Arrow and by ITEX furnished with the filter accessory. Details about the experiments, sampling time, and altitudes are found in Supplement Fig. S1.

The suitability of the particle trap for subsequent analysis was evaluated by the determination of the organic acids retained or adsorbed in the filter accessory (Sect. 3.5). Sample collection from drone at the altitude from 50 to 400 m is seen in Supplement Fig. S4. Aerosol particles were collected onto the filter attached to the ITEX unit in the drone. All the collected samples were wrapped in aluminum foil and placed into separate Minigrip bags which were stored in a freezer (-20°C) prior to analysis.

Portable BC and CPC devices were always active for measuring BC and total particle numbers during the flight of the drone. The detected BC and total particle numbers obtained with our portable devices were then compared with those obtained with reference devices at the SMEAR II station (Sect. 3.7).

2.8 Data processing and statistical analysis

Agilent ChemStation and Agilent Mass Hunter software were exploited for basic data processing, such as peak identification and integration. Mzmine2 (version 2.53) software,

Table 1. Summary of target species, sampling, and measurement techniques.

Target species	Sample phase	Sampler	Experiment(s)	Measurement technique
VOCs	Gas phase	ITEX + filter	Sect. 3.4	GC-MS
VOCs	Gas phase	SPME Arrow	Sect. 3.3, 3.4, and 3.6	GC-MS
VOCs	Particle phase	ITEX	Sect. 3.3 and 3.6	GC-MS
Carboxylic acids	Particle phase	Filter accessory	Sect. 3.5	HILIC-MS/MS
Black carbon	Particle phase	Portable AethLabs	Sect. 3.7	Real-time by portable AethLabs
Total particle number	Particle phase	Portable CPC	Sect. 3.7	Real-time portable CPC

consisting of an algorithm automated data analysis pipeline (ADAP-GC), was used for pre-processing untargeted mass spectrometric data for detection, deconvolution, and alignment of the chromatographic peaks in natural samples (Ruiz-Jimenez et al., 2019; Lan et al., 2021; Pusfitasari et al., 2022). The NIST2020 (NIST MS Search v.2.3) mass spectral database was used to check and compare the mass spectra of the aligned peaks as well as their retention indices. The identified compounds should have a spectral match of >800 and ± 45 as the maximum difference between experimental and library Kováts retention indices.

Partial least squares regression (PLSR) equations were developed for the quantification and semi-quantification of the detected compounds in natural air samples (Kopperi et al., 2013; Lan et al., 2021; Pusfitasari et al., 2022). To develop different PLSR equations for the quantification/semi-quantification of potentially identified compounds, six different concentration levels of 19 detected compounds (i.e., pyridine; *sec*-butylamine; 1-butanamine; butanenitrile; 2-propen-1-amine; diethylamine; dimethylformamide; hexylamine; trimethylamine; nonane; isobutanol; ethylacetate; methyl isobutyl ketone; hexanal; 2,3-butanedione; benzaldehyde; acetophenone; *p*-cymene; and ethyl benzene) were collected and analyzed under optimal experimental conditions. Afterwards, the data were used for the development of the PLSR equation.

Total particle numbers measured by the reference instrument, an aerosol electrometer TSI 3772 at the altitude of 4 m (ground level), were downloaded directly from the SmartSMEAR open-access database: <https://smear.avaa.csc.fi/> (last access: 6 October 2022; Junninen et al., 2009).

The measured VOC values that were collected by the ITEX sampling system and BC as well as total particle numbers at different altitudes were calculated to the same pressure level so that they could be compared to literature values (Brasseur et al., 1999; Kivekäs et al., 2009; Rajesh and Ramachandran, 2018). In this study, the reading values were corrected for ambient pressure and temperature as the following:

$$A = m_A \left[\frac{P_0 T}{P T_0} \right]^{-1}, \quad (1)$$

where A is the corrected value, m_A is the measured raw concentration, P_0 is the standard atmospheric pressure (101.3 kPa), T_0 is the standard temperature (293 K), P is the ambient atmospheric pressure, and T is the ambient temperature. Supplement Table S1 shows the data at ambient temperatures and pressures used in this study, as well as the calculated correction factors at different altitudes. In the case of VOC concentrations collected by SPME Arrows, no correction was applied since the equilibrium constant for current adsorbents and compounds was not studied at various pressures and temperatures.

3 Results and discussion

3.1 Optimization of the sampling techniques using gas chromatography–mass spectrometry

The choice of coating materials for SPME Arrow sampling systems was based on the good selectivity of MCM-41 for nitrogen-containing compounds, suitability of DVB/PDMS for most of the VOCs present in the air samples, and the capability of Carbon WR to collect volatile compounds, which cover a wide range of polarity and have a good reproducibility (Kim et al., 2020; Lan et al., 2019b; Ruiz-Jimenez et al., 2019). For the ITEX sampling system, MCM-41-TP was chosen as a sorbent material since it has proved to have good selectivity towards nitrogen-containing compounds, while TENAX-GR was selected due to its good capability to collect different VOCs present in the air (Lan et al., 2019a; Pusfitasari et al., 2022).

The optimization containing equilibrium sampling time for SPME Arrow sampling systems; breakthrough volume for the MCM-41-TP-ITEX; and desorption temperature and desorption time towards representative compounds such as diethylamine, isobutylamine, triethylamine, trimethylamine, pyridine, *p*-cymene, 2-butanol, and 2-butanone have been tested in our previous studies (Pusfitasari et al., 2022). Briefly, the average sampling time that is used before reaching equilibrium for both MCM-41-SPME Arrow and DVB/PDMS-SPME Arrow units is about 20 min. The cleaning and desorption conditions of 250 °C for 10 and 1 min, respectively, were selected to be optimal for the conditioning and analysis. The Carbon WR-SPME Arrow sampling sys-

tem was also treated in the same way in terms of conditioning and desorption methods.

In our previous study, TENAX-GR as the sorbent for the ITEX's trap accessory was able to adsorb mostly non-nitrogen-containing compounds and only a small amount of nitrogen-containing compounds (Pusfitasari et al., 2022). In the present study, universal TENAX-GR was used as the ITEX sorbent material to collect air samples. Desorption and conditioning processes were optimized using a previously developed methodology and optimal conditions similar to the MCM-41-TP-ITEX system with selective sorbent (Sect. 2.4). The repeatability of the TENAX-GR-ITEX sampler was also tested, with the relative standard deviation (RSD) between 3.4 % and 7.1 % (Supplement Tables S2 and S3), whereas the reproducibility between different ITEX units also caused by ITEX manual packing was between 4 % and 18 %.

The sampling systems used in this study needed to be stored for a certain period of time before analysis to accommodate the on-field situation. In our previous study, the sorbent in the MCM-41-TP-ITEX system could be stored at -20°C up to 18 h without losing much of the model compounds, with recoveries of around 80 % (Pusfitasari et al., 2021). For the TENAX-GR sorbent, recoveries of 98 % were obtained after storage at -20°C for 24 h but only 78 % when the sorbent was stored at room temperature for 24 h. In this study, the samples collected at the SMEAR II station had to be analyzed after storage of around 2 h since the samplers were needed for the upcoming field measurements. Therefore, both MCM-41-TP-ITEX and TENAX-GR-ITEX systems were stored at room temperature for only a few hours before the analysis.

3.2 Optimization of organic acid analysis using hydrophilic interaction liquid chromatography (HILIC)–tandem mass spectrometry

HILIC-ESI-MS/MS was employed for analysis of organic acids from filter samples. Eighteen different acids were successfully identified, and five of them were quantified using the optimized method. For the 18 model acids, the HILIC mobile phase with composition of 80 % ACN (solvent A) and 20 % of 0.05 % FA (solvent B) was chosen as the best eluent for acid separation (Supplement Table S4). The second optimized parameter was drying gas temperature, which is an important parameter in the ESI technique to allow the eluent from the HILIC column to evaporate as rapidly as possible in the ion source (Kruve, 2016). In this study, using the selected optimum eluent, i.e., ACN (80 %) and 0.05 % FA (20 %), with the flow rate of 0.25 mL min^{-1} , the drying gas temperature of 275°C was selected as the optimum temperature. Supplement Table S5 shows the established multiple reaction monitoring (MRM) method parameters for each compound using all optimized parameters including the optimized voltages for other crucial parameters, namely frag-

mentor voltage, collision energy, and cell acceleration voltage (CAV).

3.3 Application of the air-sampling system at altitudes from 50 to 400 m

In this study, the mesoporous silica-based materials, namely MCM-41 and MCM-41-TP, were used to selectively collect nitrogen-containing compounds (Lan et al., 2019b; Pusfitasari et al., 2022), whereas the commercial universal materials, TENAX-GR and DVB/PDMS, were also used to collect compounds other than nitrogen-containing compounds.

The MCM-41-TP-ITEX and TENAX-GR-ITEX sampling systems were used to collect atmospheric air samples containing both the gas phase and aerosol particles, while the samples containing only the gas phase were collected by the MCM-41-SPME Arrow and DVB/PDMS-SPME Arrow systems. The concentrations in aerosol particles were obtained via the subtraction of these results, i.e., MCM-41-TP-ITEX subtracted from MCM-41-SPME Arrow and TENAX-GR-ITEX subtracted from the DVB/PDMS-SPME Arrow.

Altogether, up to 40 VOCs were detected in the gas phase and 48 were in particle-phase samples. VOCs with various functional groups such as nitrogen-containing compounds, alcohols, ketones, aldehydes, small organic acids, and hydrocarbons were detected both by selective MCM-41-coated SPME Arrow and MCM-41-TP-ITEX sampling systems as well as by universal sorbent materials TENAX-GR-ITEX and DVB/PDMS-coated SPME Arrow systems. However, because in our previous study (Lan et al., 2019b; Pusfitasari et al., 2022), the MCM-41-SPME Arrow and MCM-41-TP-ITEX samplers gave sensitive and reliable results in selectively collecting nitrogen compounds, only the results obtained by the MCM-41-SPME Arrow and MCM-41-TP-ITEX samplers are shown for nitrogen-containing compounds in this section. Data for other VOCs were collected using ITEX, with universal sorbent materials TENAX-GR and using DVB/PDMS-coated SPME Arrow.

As can be seen from Fig. 2, eleven aliphatic amines (methylamine; dimethylamine; *sec*-butylamine; 2-propen-1-amine; 2-methyl-2-propanamine; 1-butanamine; 2-pentanamine; 1-hexanamine; *n*-hexylmethylamine; 4-heptylamine; *N*,1-dimethylhexylamine) and seven other nitrogen-containing compounds (formamide, 2-amino-1-propanol, ethylmethylcarbamate, 2-propenamide, 1H-imidazole, butanenitrile, and pyridine) were detected, quantified, and semi-quantified in the gas-phase samples with concentrations of up to 2005 ng m^{-3} . While in the particle phase (Fig. 3), a total of 16 nitrogen-containing compounds were detected with concentrations of up to 6122 ng m^{-3} . These results are comparable to our previous study in which the concentrations of nitrogen-containing compounds were up to 2930 and 5480 ng m^{-3} in the gas phase and particle phase, respectively (Pusfitasari et al.,

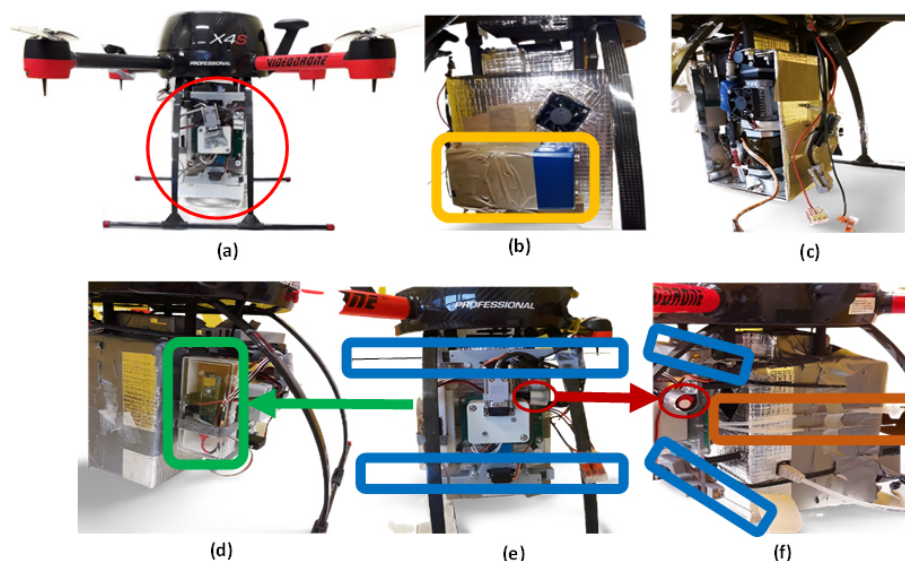


Figure 1. Drone platform sampling system with (a) air-sampling box carried by aerial drone. (b) BC placed behind the box. (c) CPC inserted into the sampling box. (d) The right side of the sampling box is a sensor that measures temperature and relative humidity. (e) Front position of the sampling box consists of SPME Arrow units (marked with blue) and a VOC sensor (red circle). (f) Sides of the sampling box include the ITEX unit and filter accessory (brown).

2022). However, the samples were collected then at altitudes from 50 to 150 m (Pusfitasari et al., 2022).

Dimethylamine, which can be produced by animal husbandry, cattle, landfill, sewage, and also industry (Ge et al., 2011), was detected in both gas and particle phase during the afternoon with concentrations up to 1004 ng m^{-3} for gas phase, and up to 5909 ng m^{-3} for the particle phase (Figs. 2a and 3a). Studies have indicated that organic amines, including dimethylamine (DMA), can be present to a large extent in the particles, e.g., by transferring from gas phase to particles (Chen et al., 2022; Zhao et al., 2007; Yu et al., 2017). DMA is one of the most common and abundant amines found in the atmosphere, and particulate DMA concentrations can increase due to enhanced biogenic VOC (BVOC) emissions and due to aerosol-phase water that increases their partition to the condensed phases (Ge et al., 2011; Youn et al., 2015; Chen et al., 2017).

Other amines that were detected at high concentrations were methylamine, pentanamine, hexanamine, hexylmethylamine, and dimethylhexylamine with concentrations up to 432, 395, 493, 340, and 1393 ng m^{-3} , respectively (Fig. 2a). For the particles, *sec*-butylamine was detected with concentrations up to 4090 ng m^{-3} , hexanamine up to 4316 ng m^{-3} , and dimethylhexylamine up to 686 ng m^{-3} (Fig. 3a).

For nitrogen-containing compounds other than amine, butanenitrile was detected with the highest concentrations up to 2005 ng m^{-3} in the gas phase and 6122 ng m^{-3} in the particle phase. 2-Amino-1-propanol, pyridine, and 1-H-imidazole were present in the gas phase as the second, third, and fourth highest concentrations up to 790, 492, and 136 ng m^{-3} , respectively. While in the particle phase, their concentrations

were up to 129, 958, and 646 ng m^{-3} , respectively. The concentrations of all detected nitrogen-containing compounds at mixed altitudes can be seen in Supplementing Table S7.

For other VOCs, 22 compounds in the gas phase (Fig. 2b) and 32 in the particle phase (Fig. 3b), containing alcohols, aldehydes, ketones, small organic acids, and hydrocarbons, were detected and quantified or semi quantified with concentrations up to 6898 ng m^{-3} in the gas phase and 8613 ng m^{-3} in the particle phase. In the gas phase, 2-methyl-1-propanol; 2,3-butanedione; *trans*-limonene oxide; methylglyoxal; acetic acid; ethyl acetate; and hexanal were discovered almost all the time during the samplings with concentrations up to 4209, 2436, 2210, 4695, 6898, 2198, and 3984 ng m^{-3} , respectively (Fig. 2b). While in the particle phase, almost all detected compounds were present in high concentrations such as 2-ethyl-1-hexanol (4114 ng m^{-3}); 2,3-butanedione (4865 ng m^{-3}); *trans*-limonene oxide (6886 ng m^{-3}); methylglyoxal (8613 ng m^{-3}); aliphatic hydrocarbons (7091 ng m^{-3}); ethyl benzene (3042 ng m^{-3}); and toluene (7715 ng m^{-3}) (Fig. 3b). Supplement Table S8 gives at mixed altitudes (50 to 400 m) the concentrations for all detected VOCs that do not belong to nitrogen-containing compounds.

In the atmosphere, 2,3-butanedione is naturally occurring in food products such as butter and beer (Boylstein et al., 2006), while *trans*-limonene oxide is detected possibly due to the partial oxidation of monoterpene limonene's olefinic bonds (Hoeben et al., 2012; Karlberg et al., 1992). Methylglyoxal, an important precursor of SOA, is produced in the atmosphere by the oxidation of hydrocarbons, such as isoprene, acetylene, toluene, and xylenes (Zhang et al., 2016; Fu

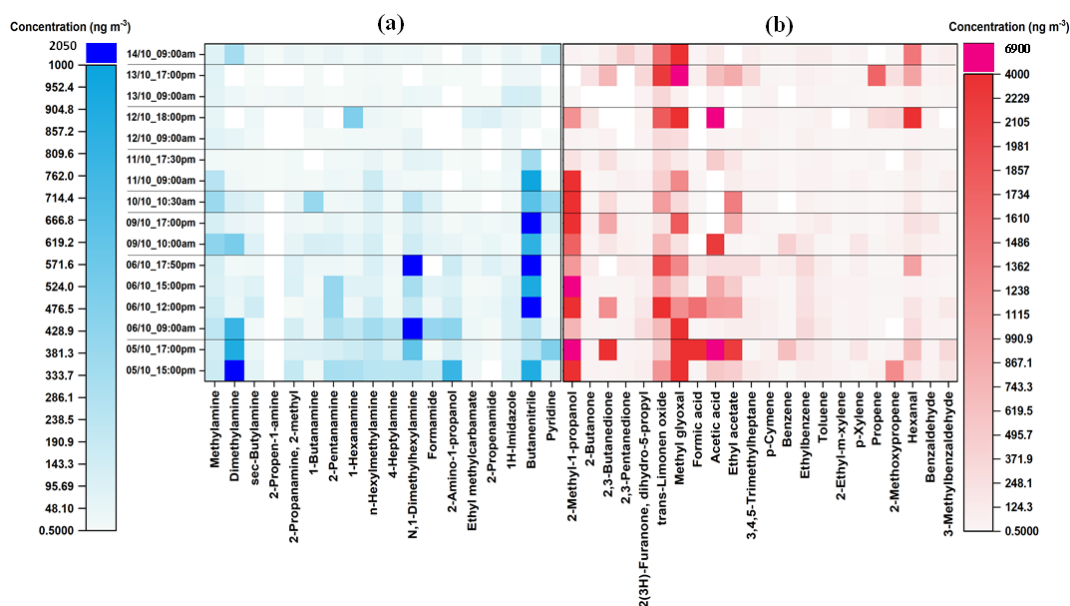


Figure 2. Concentrations of (a) nitrogen-containing compounds and (b) other VOCs in the gas-phase at the SMEAR II station, Hyttiälä, at mixed altitudes between 50 and 400 m. (a) Nitrogen-containing compounds were collected using the MCM-41-SPME Arrow system with selective sorbent, while (b) other VOCs were collected using the DVB/PDMS-SPME Arrow system with universal sorbent. White color represents not detected.

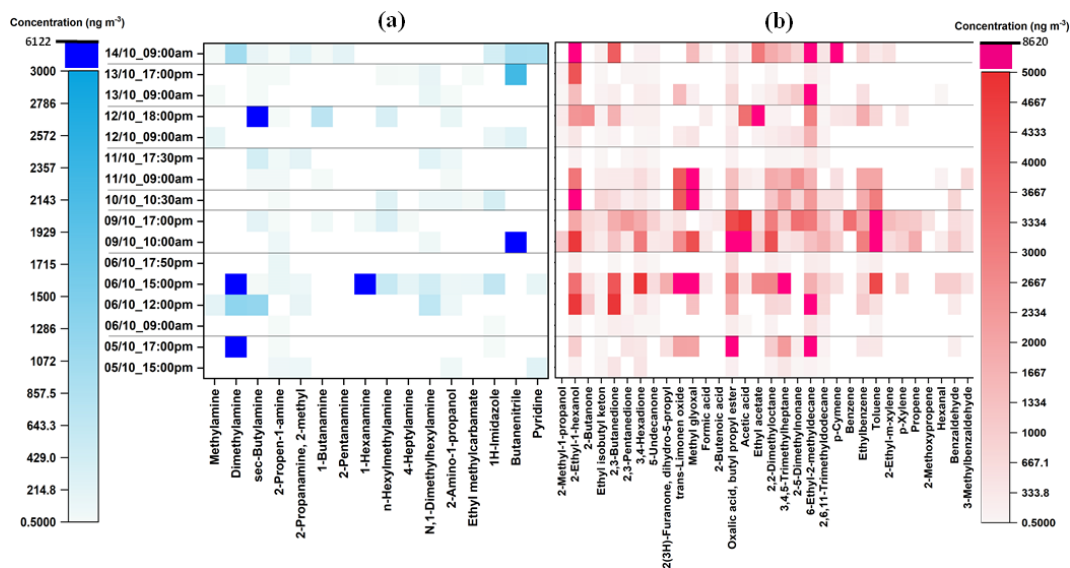


Figure 3. Concentrations of (a) nitrogen-containing compounds and (b) other VOCs in the particle phase at SMEAR II station, Hyttiälä, at the mixed altitude between 50 and 400 m. Samples were collected using the MCM-41-TP-ITEX system with selective sorbent (a) and TENAX-GR-ITEX systems with universal sorbent (b). White color represents not detected.

et al., 2013; Olsen et al., 2007). Other detected compounds, e.g., acetic acid and ethyl acetate, can be released from different sources such as biomass burning and vegetation (Rosado-Reyes and Francisco, 2006; Khare et al., 1999).

The diurnal pattern in both gas and particle phases was also observed. As can be seen from Fig. 2 in the gas phase, aliphatic amines that are mostly emitted by biogenic sources

were present in lower concentrations in the evening (started at 17:00 LT) compared to daytime, whereas some amines, namely hexanamine and dimethylhexylamine, had slightly higher concentrations in the evening. These results agree well with our previous study in which most of the amines had a diurnal variation with a daytime maximum due to their dependency on temperature for their emission, indicating the

contribution to biogenic sources (Pusfitasari et al., 2022). High concentrations of some amines in the evenings could be caused by the weak atmospheric mixing at night, resulting in decreased reactions with atmospheric acids (Hemmilä et al., 2018). In contrast, VOCs that were emitted from other sources had higher concentrations mostly in the afternoons, except for non-nitrogenated compounds with high concentrations also in the mornings on 11 October 2021. The anthropogenic sources that might affect this result were probably carried by the wind from other places and were mixed in the atmosphere since the samples were collected at high altitudes (up to 400 m). In the particle phase, there was no clear pattern seen since our samples were mostly collected only in the mornings and late afternoons. However, in our previous study we found that VOCs had high concentrations in mornings and evenings since temperature dependency affects the deposition of amines in the colder evenings, and then they partition back to the atmosphere in the higher-temperature mornings (Pusfitasari et al., 2022). In this present study, we can also see from Fig. 3 high concentrations in both the mornings and late afternoons but surprisingly also at noon (on 6 October).

The correlation among all the VOCs in both gas and particle phases was also studied. An R value close to one and a P value of <0.05 mean that there is a correlation between variables. As can be seen from Supplement Fig. S5, only a few compounds in the gas phase correlate with those detected in the particle phase, such as particulate benzaldehyde that correlated with alcohol vapors (i.e., gas-phase of 2-methyl-1-propanol and 2-ethyl-1-hexanol) and some amines (i.e., methylamine, *sec*-butylamine, 2-pentanamine, and *n*-hexylmethylamine). These correlations can be explained by the studies conducted by Perez et al. (2017), who were investigating the implication of aldehyde–amines for aerosol growth by providing low-energy neutral pathways for the formation of larger and less-volatile compounds (Perez et al., 2017).

In addition, we can also see that some nitrogen-containing compounds correlated with aliphatic hydrocarbons, aliphatic carbonyl, and aliphatic alcohols in the gas phase, indicating that they might be emitted from the same sources. This finding is supported by the study conducted by Isidorov et al. (2022). Although their group could not detect selectively nitrogen-containing compounds as they used universal sorbent material for the collection of air sample (i.e., DVB/CAR/PDMS-SPME), they could detect all other VOC compounds at the same time from the boreal forest (Isidorov et al., 2022).

3.4 Evaluation of ITEX filter accessories

In our previous study, it was proved that a small filter can be used to trap particles, allowing only the gas phase to enter the ITEX sampler (Pusfitasari et al., 2022; Ruiz-Jimenez et al., 2019). The experiments were properly designed to check and

compare the results achieved for gas-phase compounds using a passive SPME Arrow sampling system and an active ITEX plus filter sampling system. In the present study, the samples were collected from 11 to 14 October 2021, and TENAX-GR-ITEX was exploited with the filter accessory. The altitudes for these experiments were 50–400 m (Supplement Fig. S1). As can be seen in Supplement Fig. S6, aliphatic amines were the major nitrogen-containing compounds detected in both the gas and particle phases. For VOCs without any nitrogen compounds, following the results in the previous section (i.e., Sect. 3.3), alcohols, ketones, aldehydes, organic acids, and some hydrocarbons were detected, quantified, and semi-quantified with the concentrations shown in Supplement Fig. S6. The results of the gas-phase compounds sampled by the ITEX system with the filter accessory were comparable with the gas-phase results obtained by the SPME Arrow sampling system.

In addition to the comparison of the gas phase collected by the ITEX furnished with the filter accessory with the SPME Arrow system, the compound recoveries of the gas phase obtained by the first ITEX sampling system furnished with the filter were also evaluated. The recoveries of non-polar compounds, such as alkanes, were only $<50\%$ (Supplement Table S9). The more polar compounds, such as alcohols, acids, and nitrogen-containing compounds, were mostly detected at higher recoveries from 50% up to 99% . Most probably, non-polar compounds of the gas phase were partly adsorbed to the ITEX filter accessory that was made from PTFE (Parshintsev et al., 2011). PTFE has a non-polar structure due to the distribution of the fluorine atom around the carbon polymer backbone, which balances the electronegative and electropositive charges (Parsons et al., 1992). Hence, our study proved that the ITEX sampling systems with PTFE filter are not only good at trapping aerosol particles but also excellent at collecting polar compounds, such as nitrogen-containing compounds, of the gas phase. Nevertheless, since nitrogen-containing compounds are very water soluble, the humidity level in the air will most likely affect the distribution of polar compounds between the filter and the ITEX adsorbent, e.g., water condensing to the filter at high humidity.

3.5 Analysis of aerosol particles collected by ITEX with PTFE filter using liquid chromatography tandem mass spectrometry

Filter-collected aerosol particles in the ITEX system were extracted and analyzed separately by using HILIC-MS/MS to quantify carboxylic and dicarboxylic acids, since most organic acids cannot be analyzed by GC without derivatization, except small organic acids such as formic acid and acetic acid. The organic acids have a capability to significantly enhance the hygroscopicity of aerosol particles and contribute to the acidity of precipitation and cloud water.

As can be seen in Table 2, five main acids (succinic acid, benzoic acid, phthalic acid, glutaric acid, and adipic acid)

were identified and quantified. Succinic acid was observed in almost every sample, and its higher prevalence could possibly be explained by the fact that it can be formed from common biogenic and anthropogenic precursors such as isoprene and toluene (Sato et al., 2021). The aromatic acids such as benzoic acid and phthalic acid were also detected in the samples. The concentrations of benzoic acid (up to $1.4 \mu\text{g m}^{-3}$) were higher than those of phthalic acid (up to $0.77 \mu\text{g m}^{-3}$). Observation of these acids is relevant as their aromatic hydrocarbon precursors are common in the atmosphere. In addition, phthalic acid has also been detected in the summer 2012 samples, but then no benzoic acid was detected in the gas phase or particulate phase (Kristensen et al., 2016).

Glutaric and adipic acids were also determined from samples taken on 11 and 14 October. Glutaric acid and adipic acid have been commonly detected in atmospheric aerosols and cloud droplets (Wen et al., 2021). Other dicarboxylic acids, such as glycolic acid and *cis*-pinonic acid were detected in only one sample in which their limits of detection (LODs) were exceeded (Supplement Table S10). The possible reason for the low concentration of glycolic acid might be that it can be formed as an oxidation product of biogenic isoprene (Liu et al., 2012).

3.6 Comparison of nitrogen-containing compounds and other VOCs at altitudes of 50 and 400 m

The aim of this study was to compare the composition of VOCs at altitudes of 50 and 400 m, separately. Carbon WR-SPME Arrow unit with universal sorbent was used to collect a wide range of VOCs in the gas phase. MCM-41-TP-ITEX and TENAX-GR-ITEX sampling systems were employed to collect gas and particle phases.

As can be seen from Fig. 4, the concentrations of amines that were emitted by biogenic sources, such as methylamine, dimethylamine, *sec*-butylamine, butanamine, pentanamine, hexylmethylamine, and heptylamine, were mostly found at higher concentrations at the lower altitude (50 m). The concentrations were decreased at higher altitude (400 m), most probably due to the dilution (since the sources are on the ground) and reaction with hydroxyl radical (Kieloaho, 2017).

For nitrogen-containing compounds other than amines, imidazole was one of the compounds detected by our system. There have been a number of laboratory studies where imidazole has been reported to be the major product of glyoxal reaction with ammonium ions or primary amines on secondary organic aerosol. In addition, imidazoles can become a secondary product of the reaction of dicarbonyls with nitrogen-containing compounds; therefore, they might have the potential to act as photosensitizers, triggering secondary organic aerosol growth and forming constituents of light-absorbing brown carbon (De Haan et al., 2011; Dou et al., 2015; Teich et al., 2020). Imidazoles were detected mostly in the particle phase with concentrations up to 422 ng m^{-3} at 50 m and 338 ng m^{-3} at 400 m. Slightly lower concentrations were dis-

covered in the gas phase with values up to 58 ng m^{-3} at an altitude of 50 m and 510 ng m^{-3} at an altitude of 400 m.

Other nitrogen-containing gas-phase compounds detected, such as formamide, 2-amino-1-propanol, ethylmethylcarbamate, and propenamide, also showed the same pattern with higher concentrations at 400 m compared to 50 m. These compounds were most probably transported by the wind from other areas and emitted by various sources, such as biomass burning, peatland, industries, and other anthropogenic sources (Pusfitasari et al., 2022).

As can be seen from Fig. 5, gas-phase VOC compounds without nitrogen, such as *trans*-limonene oxide, methylglyoxal, hexanal, and ketones, have higher concentrations at an altitude of 400 m compared to 50 m; whereas some acids, such as acetic acid and formic acid, ethyl acetate, and BTX (benzene, toluene, xylene) were mostly discovered at the altitude of 50 m. In the case of alcohols, they had comparable concentrations at both 50 and 400 m. In the particle phase, most of the compounds had higher concentrations at 400 m than at 50 m, except for some hydrocarbons (such as 2,5-dimethylnonane and 6-ethyl-2-methyldecane) that had high concentrations at 50 m.

Alcohols are a prevalent class of VOCs in the atmosphere and can be emitted by biogenic sources such as rain forest and also from anthropogenic sources such as alcohol-gasoline-blended fuel and industries (Nguyen et al., 2001; McGillen et al., 2017). Therefore, it is no wonder that in this study alcohol was found at almost all altitudes. The alcohol emission is becoming a concern since it can react with Criegee intermediates (product of biogenic alkenes oxidized by ozone) to produce α -alkoxyalkyl hydroperoxides (AAHs) that can lead to the formation of secondary organic aerosols (Dussault and Sahli, 1992; Bonn et al., 2004; McGillen et al., 2017).

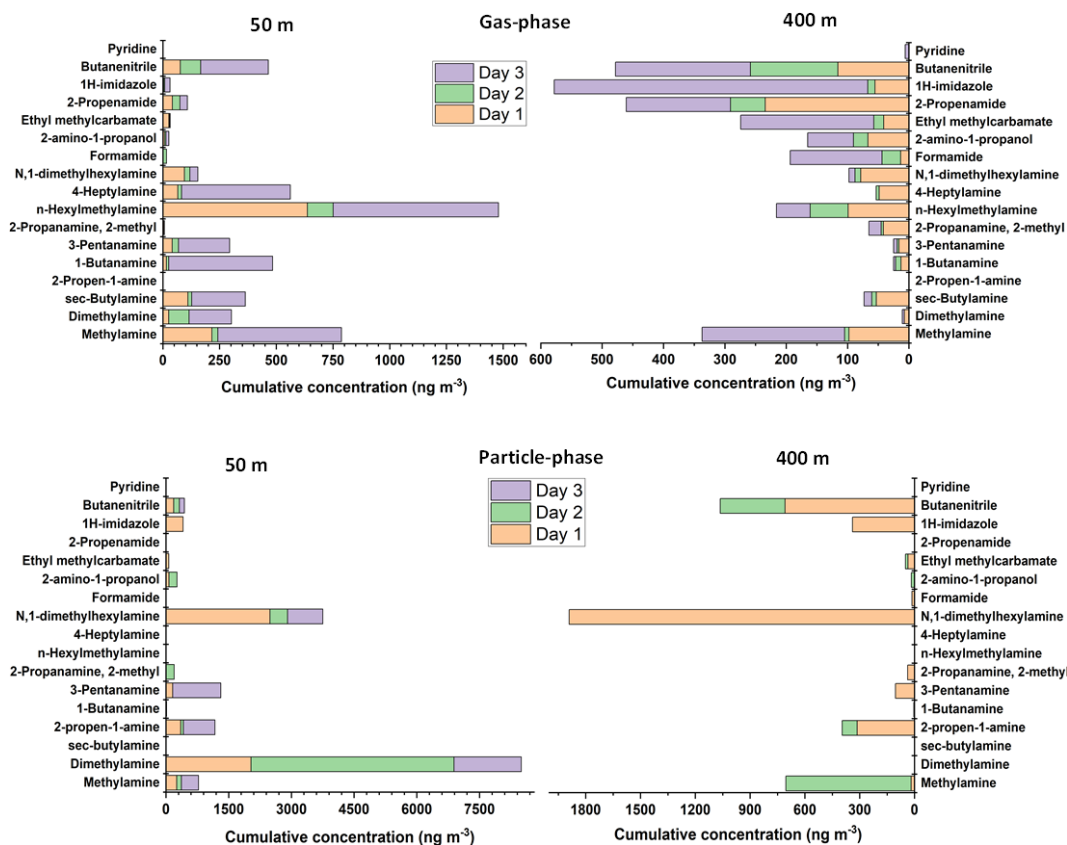
In the gas-phase samples, benzene, toluene, and *p*-xylene (BTX) were found mostly at the altitude of 50 m with concentrations up to 219, 410, and 70 ng m^{-3} , respectively. Since BTX can be emitted from gasoline (major fuel of vehicles) and the samples were collected close to the parking area, the higher concentrations were found at lower altitude (50 m). This finding is comparable with the study conducted by Chen et al. (2018), who measured the BTX concentrations between 100 and 300 ng m^{-3} from forest canopy at altitudes between 20 and 26 m (Chen et al., 2018; Yassaa et al., 2006). Toluene and *p*-xylene were also detected in the particle phase as VOCs may be adsorbed onto the surface of the particles (Dehghani et al., 2018; Kamens et al., 2011). The higher concentrations were detected at an altitude of 400 m with concentrations of up to 539 and 2475 ng m^{-3} for toluene and *p*-xylene, respectively. BTX plays an important role in the atmosphere since it has been recognized as an important photochemical precursor for secondary organic aerosol (Correa et al., 2012; Ng et al., 2007).

Aldehydes in the atmosphere are also of concern because of their heterogeneous reaction with acids affecting parti-

Table 2. Concentrations of acids collected from the ITEX filters at altitudes of 50–400 m.

Sampling time	Succinic acid (ng m ⁻³)	Benzoic acid (ng m ⁻³)	Phthalic acid (ng m ⁻³)	Glutaric acid (ng m ⁻³)	Adipic acid (ng m ⁻³)
11 Oct 2021	1416	1416	657	1619	10 926
12 Oct 2021	435–789	1416	769	n.d.	n.d.
13 Oct 2021	496–4654	n.d.	n.d.	n.d.	n.d.
14 Oct 2021	n.d.	n.d.	n.d.	1720	6374

* n.d. represents not detected

**Figure 4.** Concentrations of nitrogen-containing compounds in the gas phase and particle phase at SMEAR II station at altitudes of 50 and 400 m for 3 d (8 to 10 October 2021). For the gas-phase samples were collected using Carbon WR-SPME Arrow sampling system, and the particle-phase samples were collected by MCM-41-TP-ITEX system. The concentrations of aerosol particle compounds were obtained via subtraction the results obtained by MCM-41-TP-ITEX from those obtained by the Carbon WR-SPME Arrow with universal sorbent.

cle growth (Jang and Kamens, 2001; Altshuler, 1993). In our study, some aldehydes, such as methylglyoxal, hexanal and benzaldehyde, were found in both the gas and particle phases at the altitude of 400 m in higher concentrations than at the altitude of 50 m. At the altitude of 400 m, methylglyoxal was the most abundant aldehyde with concentrations up to 580 ng m⁻³ in the gas phase and 1418 ng m⁻³ in the particle phase. Ketones in aerosol particles have been associated with burning and non-burning forest, and it represented up to 27 % of the current organic aerosol mass concentration (OM) (Takahama et al., 2011). Ketones were also found in

this study at higher concentrations at high altitude (400 m) in both gas phase and particle phase.

The last group of chemicals that was detected by our collection systems was small organic acids and from these especially formic acid and acetic acid. Organic acids have an important role as chemical constituents in troposphere, and they contribute with a large fraction (25 %) to the non-methane hydrocarbons in the atmosphere. The organic acids contribute to the acidity of precipitation and cloud water (Khare et al., 1999). Acetic acid was found in both gas and particle phases at altitudes of 50 and 400 m. However, the amount of

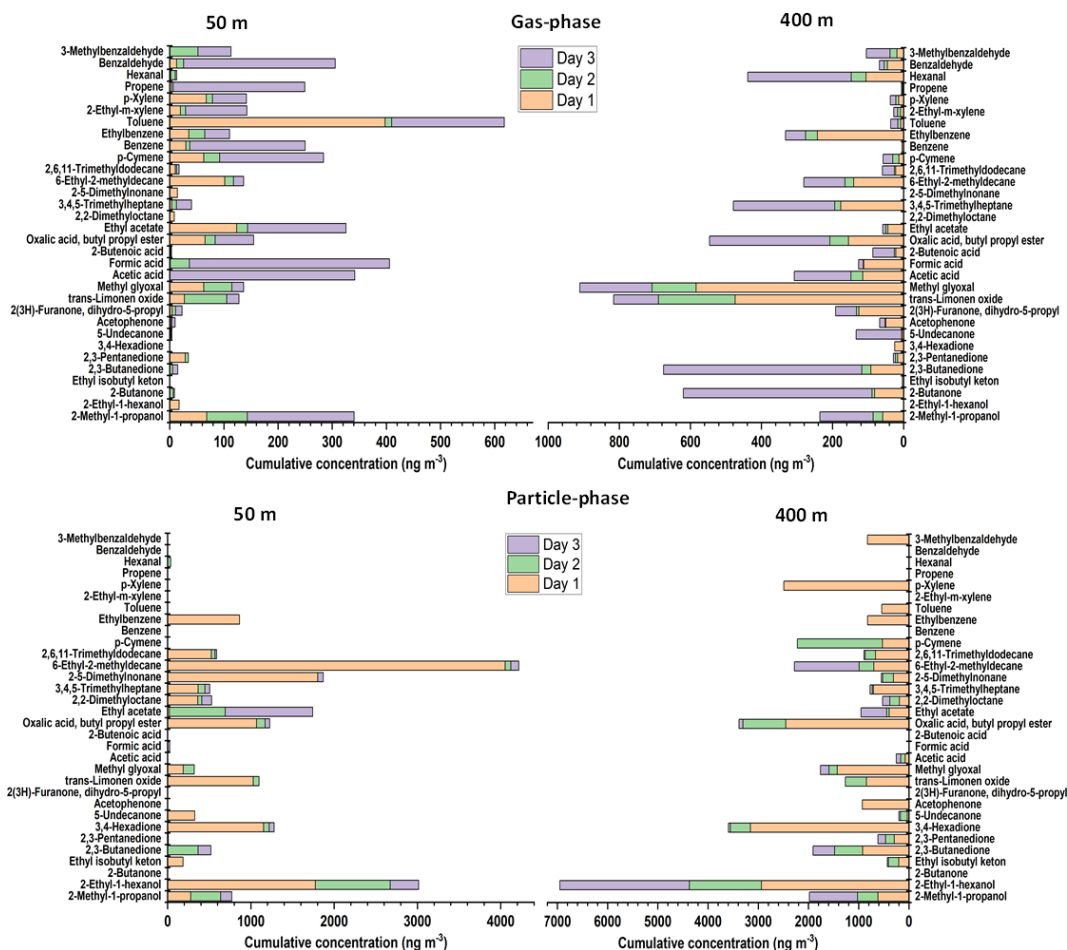


Figure 5. Concentrations of non-nitrogenated VOC compounds in the gas phase and in the particle phase at SMEAR II station at altitudes 50 and 400 m for 3 d (8 to 10 October 2022). The gas-phase samples were collected using Carbon WR-SPME Arrow system, and particle-phase samples using TENAX-GR-ITEX sampling systems. The concentrations of aerosol particle compounds were obtained via subtraction the results obtained by TENAX-GR-ITEX from those obtained by the Carbon WR-SPME Arrow with universal sorbent.

both formic acid and acetic acid found in the gas phase was higher than that in the particle phase. These acids can originate from various sources such as vehicular emissions, ants, plants, soil, and biomass burning (Zhang et al., 2022).

3.7 Evaluation of total particle numbers and black carbon at high altitudes. Portable CPC and BC devices carried by aerial drone

The particle number concentration and BC concentration were measured by using portable CPC and BC measurement devices carried by the drone. The BC concentration was measured at 880 nm wavelength (near IR), as at this wavelength BC has strong absorption and least interference by other organic molecules (Dumka et al., 2010). The results were compared to those measured by the reference instruments at the SMEAR II station. The correction factors to the same pressure level as described in Sect. 2.8 were calculated with the values between 0.994 and 1.035 (Supplement Table S1). Sup-

plement Fig. S7 for CPC proves a correlation between the results obtained by our portable CPC and reference instrument, with direct linear correlation close to 1 (R^2 of 0.9564). Oppositely, linear correlation for BC was only 0.2492, indicating that there was no correlation between the reference instruments and our BC meter in the drone.

Our portable BC monitor in the drone gave higher concentration values than the reference one, located at 4 m. The reasons for the differences could be caused by amplification factor that raised due to multiple scattering in the quartz fiber matrix of the tape of the Aethalometer. The deposition of scattering material along with BC to the filter tape produced the “shadowing effect”, causing the BC meter to show higher concentration values (Weingartner et al., 2003; Dumka et al., 2010). Alternatively, the differences can be explained by different measurement altitudes between the reference instrument (measured at 4 m) and BC monitor in the drone (up to 400 m). At lower altitude, living activities such as heating sauna and fuel burning from cars nearby the area might

contribute to the results, while at higher altitudes BC long distance transport contributes to the results as well (Meena et al., 2021). The atmospheric boundary layer height (ABLH) also plays an important role to govern concentration of BC at high altitudes since it can affect pollutant aggregation, transmission, wet deposition, and dry sedimentation (Meena et al., 2021). The boundary layer (BL) is the lowest part of troposphere and connects the ground and the free atmosphere. The average boundary layer height at the Hyytiälä SMEAR II station in autumn (October) was around 500 m (Sinclair et al., 2022), explaining why we found higher BC concentration at high altitudes. For comparison, Table 3 shows the BC mass concentrations measured at high altitudes in different areas.

Autumn average of BC pollution in Hyytiälä according to Hyvärinen et al. (2011) was about 1291 ng m^{-3} , while Hienola et al. (2013) reported the October average was 550 ng m^{-3} (Hyvärinen et al., 2011; Hienola et al., 2013). However, those studies were conducted using reference instrument at low altitude, i.e., 4 m above the ground.

The drone stability was evaluated during the vertical and horizontal movements (drone movement schematic is showed in Supplement Fig. S4). Figure 6 shows that the BC concentration and total particle numbers were affected by the drone movements. Rapid ascending (area number I) affected both BC and CPC. BC measurements showed negative values when the drone started to warm up, take off, and then quickly move vertically with a speed of 2.5 m s^{-1} . These readings could be due to the temperature change on the BC sensor when the drone was ready to take off and the drone's fast ascent (Pan et al., 2011; Elomaa, 2022). The portable CPC device also gave fluctuating data. Both BC and CPC devices started to stabilize when approaching an altitude of 365 m.

At the beginning of drone vertical movement at the altitude of 400 m, the portable CPC gave more stable results when the speed was decreased and when it was allowed to stabilize for 30 s (as can be seen in area number II), resulting in smooth changes in the total particle numbers and some deviations at each altitude. However, BC concentration varied also with high standard deviations at high altitude without any specific movement, indicating that the drone movement influenced the portable BC device. Pan et al. (2011) have suggested that a large variation in the BC measurements could be caused by several factors such as boundary layer stratification and turbulence. In addition, the BC sensor was also very sensitive to a change in temperature. They observed that the BC concentration could change quickly only after a short period of sunshine. Based on the standard deviations, horizontal movements (area numbers III and IV) affected the portable CPC much less compared to the portable BC.

It can be seen from the results of Fig. 7 that (for the 3 measurement days) BC and CPC devices had similar patterns at all altitudes (100, 200, 300, and 400 m). The daily means of total particle numbers are found in Supplement Table S12. Although the concentrations at an altitude of 400 m seem to be slightly lower than those detected at lower altitudes, the

patterns of total particle number are similar at every altitude (Fig. 7), most possibly due to the limited anthropogenic activities near the sampling site. The potential mixing and the particle formation in the atmosphere most likely influenced the total particle number detected. In addition, particulate long-range transport from different areas could also affect the total particle concentration in the air (Casquero-Vera et al., 2020).

Figure 7 also demonstrates that the diurnal pattern was different, revealing that the particle concentrations at different times of the day were influenced by different sources compared to BC. Almost at all altitudes, the diurnal variation for day 1 and day 2 included a late afternoon peak at 17:00 LT. The particle concentrations increased significantly on day 3, especially during the first and second samplings before the change to lower concentrations. The samplings for the first 2 measurement days were carried out during the weekend without many activities that produce VOCs, which is opposite to Monday morning when normal working activities close to sampling area were going on.

In contrast to the pattern of total particle numbers, the daily average of BC concentration during the measurement time period was increased at higher altitudes (Supplement Table S12), indicating that the BC pollutant was distributed from different areas. These trends agree well with the earlier studies (Tripathi et al., 2007). Figure 7 shows that the BC diurnal pattern was similar with that of total particle numbers, except on day 2 when BC concentration decreased significantly at 13:30 LT, excluding the altitude of 200 m. However, BC concentration increased again at 17:00 LT most likely due to, for example, sauna heating and air mixing following long-range transport from different areas.

During the measurement time, BC at high altitudes (400 m) and total particle numbers at all altitudes (100–400 m) showed a diurnal cycle with a peak observed on Monday morning at 09:00 LT, possibly due to morning traffic and/or wind-driven pollution transport as suggested by previous studies (Bonasoni et al., 2010; Sandeep et al., 2022). The high BC concentration at high altitude, especially at 400 m, was mostly caused by long-range transport and the atmospheric boundary layer height as discussed earlier, and BC and also other particles contributed to the total particle numbers.

4 Conclusions

An aerial drone carrying the reliable and versatile miniaturized air-sampling systems SPME Arrow and ITEX as well as portable BC and CPC devices was successfully used for the collection of air samples. Up to 48 VOCs were detected in gas-phase and particle-phase samples, and their distribution at altitudes from 50 to 400 m was studied. Some differences between VOC compositions at altitudes of 50 and 400 m could be explained by the different sources of the

Table 3. Average BC concentrations observed at different locations.

Location	Altitude	Environment	Average BC concentration (ng m ⁻³)	Reference
Hyytiälä, Finland	100 m	Boreal forest	2278 ± 1188	This study
Hyytiälä, Finland	200 m	Boreal forest	2500 ± 1497	This study
Hyytiälä, Finland	300 m	Boreal forest	3564 ± 1648	This study
Hyytiälä, Finland	400 m	Boreal forest	3909 ± 729	This study
Hyytiälä, Finland	4 m	Boreal forest	320–1291 ± 337*	Hyvärinen et al. (2011)
Mahabaleswar, India	1378 m	Rural	2600 ± 260	Meena et al. (2021)
Mountain Huang, China	1840 m	Rural	1663 ± 919	Pan et al. (2011)
Port Blair, India	73 m	Rural	2446 ± 66	Moorthy and Babu (2006)
Sinhagad, India	1300 m	Rural	1500	Safai et al. (2007)

* 320 ng m⁻³ was the annual average, while 1291 ng m⁻³ was the concentration average measured during the pollution event in autumn.

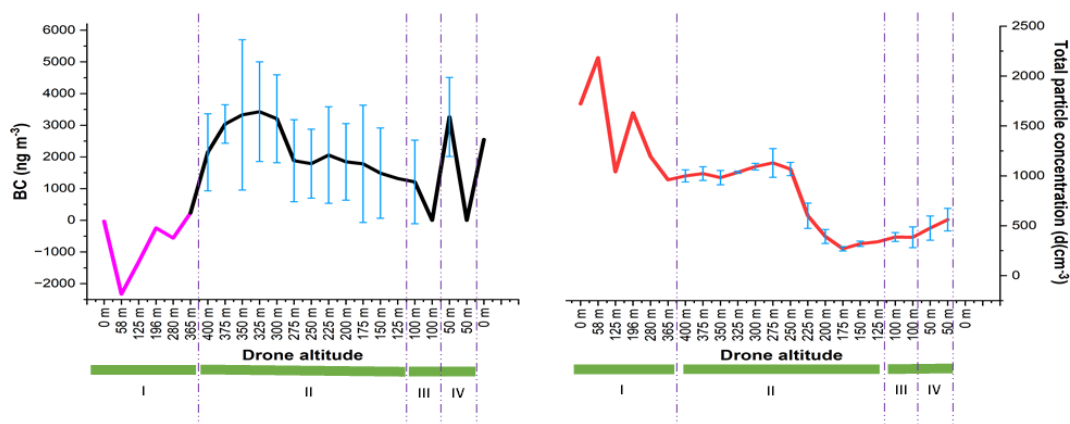


Figure 6. Evaluation of drone's vertical and horizontal movements. I indicates that the drone is moving up with the speed of 2.5 m s⁻¹. II indicates that the drone is descending with the speed of 1.25 m s⁻¹ to each altitude before staying for 30 s. III and IV indicate the horizontal movement to 100 m far away, with a speed of 5 m s⁻¹.

VOC emissions. The compounds that most probably originate from the same source had a linear correlation, as well as the compounds that were present in both gas-phase and particle-phase samples. The capability of the ITEX sampler, furnished with the filter accessory, for the collection of gas-phase samples, was evaluated by comparing it with the SPME Arrow sampling system, resulting in high agreement, especially for polar compounds with recoveries up to 99%. In contrast, non-polar compounds gave low recoveries due to the *like dissolves like* rule, meaning that non-polar compounds might be adsorbed to the non-polar PTFE filter of the ITEX sampling system.

The portable CPC gave comparable results with those obtained by the conventional reference CPC instruments at the SMEAR II station, which is opposite to the portable BC device that was affected by the drone's vertical and horizontal movements. The total particle number and BC data gave similar diurnal patterns, indicating that they were correlated. The pattern was observed during the weekend. The highest con-

centrations were found during times with human activities. The distribution was also similar to VOCs that were produced by anthropogenic sources and found in high-altitude samples, since the wind most probably carried the VOCs from other sites. For the spatial distribution pattern, BC concentrations were increased at higher altitudes due to long-range transport and the atmospheric boundary layer height. The total particle numbers, affected by the similar factors, varied more depending on the sources. This can be explained by the different VOCs that contributed to the particle formations and the particle sizes measured by the portable CPC and BC monitors.

Overall, our study described a drone equipped with miniaturized air sampling techniques. SPME Arrow and ITEX together with portable BC and CPC devices were used for the collection of atmospheric VOCs and for the measurement of BC and total number of particles at high altitudes. To further improve the reliability of the results in the future, a portable BC monitor that includes a better electronic model

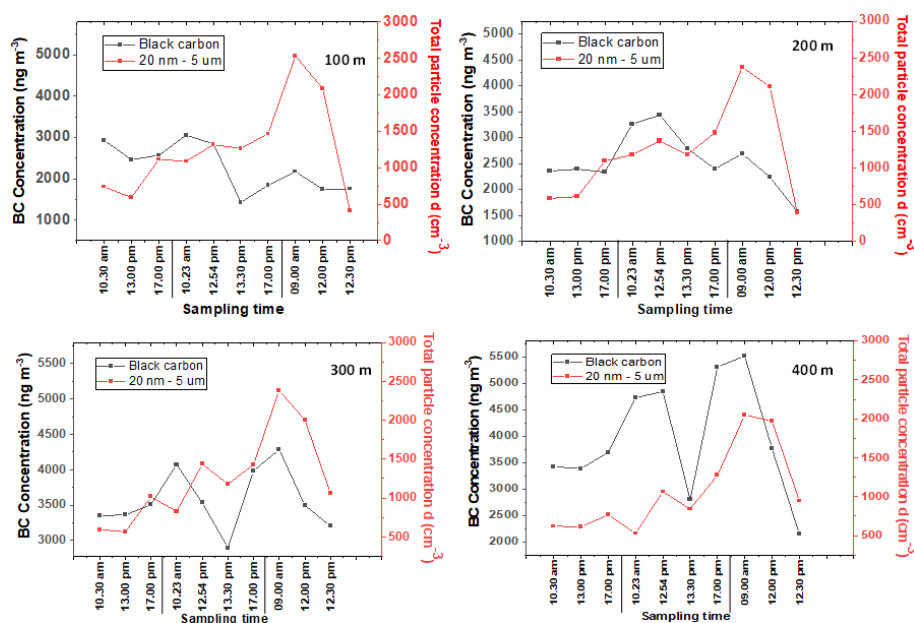


Figure 7. Time series evaluation of CPC and black carbon at the heights of 100, 200, 300, and 400 m. Sampling was conducted on October 9 (Day 1), 10 (Day 2), and 11 (Day 3), 2021. The values and point averages are shown in Supplement Table S11.

and the possibility to adjust the device position in the drone are needed.

Data availability. Data used in this work are available from the authors upon request (kari.hartonen@helsinki.fi, marja-liisa.riekkola@helsinki.fi).

Supplement. The supplement related to this article is available online at: <https://doi.org/10.5194/acp-23-5885-2023-supplement>.

Author contributions. EDP, JRJ, JH, KH, MJ, TP, and MLR designed the experiments. EDP, AT, MS, and JRJ carried out the experiments. EDP performed data interpretation and visualization. JRJ performed the statistical analysis. YW, JH, JK, and KL were responsible for CPC and BC hardware, software, and reference data. EDP, JRJ, KH, TP, and MLR prepared the manuscript with contributions from other co-authors.

Competing interests. At least one of the (co-)authors is a member of the editorial board of *Atmospheric Chemistry and Physics*. The peer-review process was guided by an independent editor, and the authors also have no other competing interests to declare.

Disclaimer. Publisher's note: Copernicus Publications remains neutral with regard to jurisdictional claims in published maps and institutional affiliations.

Acknowledgements. Financial support was provided by the Jane and Aatos Erkkö Foundation and Academy of Finland (ACCC flagship “Finnish Research Flagship” grant no. 337549). CTC Analytics AG (Zwingen, Switzerland) and BGB Analytik AG (Zürich, Switzerland) are thanked for the cooperation. Tapio Elomaa is also acknowledged for the fruitful discussion, especially about black carbon (BC) and condensation particle counters (CPCs). In addition, we also thank the staff of the SMEAR II station, Hyytiälä, for the valuable help.

Financial support. This research has been supported by the Jane ja Aatos Erkon Säätiö (Quantifying carbon sink, CarbonSink+ and their interaction with air quality grant) and the Academy of Finland (grant no. 337549).

Open-access funding was provided by the Helsinki University Library.

Review statement. This paper was edited by Theodora Nah and reviewed by two anonymous referees.

References

- Ahlberg, E., Falk, J., Eriksson, A., Holst, T., Brune, W. H., Kristensson, A., Roldin, P., and Svenningsson, B.: Secondary organic aerosol from VOC mixtures in an oxidation flow reactor, *Atmos. Environ.*, 161, 210–220, <https://doi.org/10.1016/j.atmosenv.2017.05.005>, 2017.
- Almeida, J., Schobesberger, S., Kürten, A., Ortega, I. K., Kupiainen-Määttä, O., Praplan, A. P., Adamov, A., Amorim, A.,

- Bianchi, F., Breitenlechner, M., David, A., Dommen, J., Donahue, N. M., Downard, A., Dunne, E., Duplissy, J., Ehrhart, S., Flagan, R. C., Franchin, A., Guida, R., Hakala, J., Hansel, A., Heinritzi, M., Henschel, H., Jokinen, T., Junninen, H., Kajos, M., Kangasluoma, J., Keskinen, H., Kupc, A., Kurtén, T., Kvashin, A. N., Laaksonen, A., Lehtipalo, K., Leiminger, M., Leppä, J., Loukonen, V., Makhmutov, V., Mathot, S., McGrath, M. J., Nieminen, T., Olenius, T., Onnela, A., Petäjä, T., Riccobono, F., Riipinen, I., Rissanen, M., Rondo, L., Ruuskanen, T., Santos, F. D., Sarnela, N., Schallhart, S., Schnitzhofer, R., Seinfeld, J. H., Simon, M., Sipilä, M., Stozhkov, Y., Stratmann, F., Tomé, A., Tröstl, J., Tsigogeorgas, G., Vaattovaara, P., Viisanen, Y., Virtanen, A., Vrtala, A., Wagner, P. E., Weingartner, E., Wex, H., Williamson, C., Wimmer, D., Ye, P., Yli-Juuti, T., Carslaw, K. S., Kulmala, M., Curtius, J., Baltensperger, U., Worsnop, D. R., Vehkamäki, H., and Kirkby, J.: Molecular understanding of sulphuric acid-amine particle nucleation in the atmosphere, *Nature*, 502, 359–363, <https://doi.org/10.1038/nature12663>, 2013.
- Altshuller, A. P.: Production of aldehydes as primary emissions and from secondary atmospheric reactions of alkenes and alkanes during the night and early morning hours, *Atmos. Environ. A-Gen.*, 27, 21–32, [https://doi.org/10.1016/0960-1686\(93\)90067-9](https://doi.org/10.1016/0960-1686(93)90067-9), 1993.
- Anenberg, S. C., Schwartz, J., Shindell, D., Amann, M., Faluvegi, G., Klimont, Z., Janssens-Maenhout, G., Pozzoli, L., van Dingenen, R., Vignati, E., Emberson, L., Muller, N. Z., Jason West, J., Williams, M., Demkine, V., Kevin Hicks, W., Kuylensstierna, J., Raes, F., and Ramanathan, V.: Global air quality and health co-benefits of mitigating near-term climate change through methane and black carbon emission controls, *Environ. Health Persp.*, 120, 831–839, <https://doi.org/10.1289/ehp.1104301>, 2012.
- Asbach, C., Schmitz, A., Schmidt, F., Monz, C., and Todea, A. M.: Intercomparison of a personal CPC and different conventional CPCs, *Aerosol Air Qual. Res.*, 17, 1132–1141, <https://doi.org/10.4209/aaqr.2016.10.0460>, 2017.
- Bonasoni, P., Laj, P., Marinoni, A., Sprenger, M., Angelini, F., Arduini, J., Bonafè, U., Calzolari, F., Colombo, T., Decesari, S., Di Biagio, C., di Sarra, A. G., Evangelisti, F., Duchi, R., Facchini, M.C., Fuzzi, S., Gobbi, G. P., Maione, M., Panday, A., Roccatto, F., Sellegri, K., Venzac, H., Verza, G. P., Villani, P., Vuillermoz, E., and Cristofanelli, P.: Atmospheric Brown Clouds in the Himalayas: first two years of continuous observations at the Nepal Climate Observatory-Pyramid (5079 m), *Atmos. Chem. Phys.*, 10, 7515–7531, <https://doi.org/10.5194/acp-10-7515-2010>, 2010.
- Bonn, B., von Kuhlmann, R., and Lawrence, M. G.: High contribution of biogenic hydroperoxides to secondary organic aerosol formation, *Geophys. Res. Lett.*, 31, 1–4, <https://doi.org/10.1029/2003GL019172>, 2004.
- Boylstein, R., Piacitelli, C., Grote, A., Kanwal, R., Kullman, G., and Kreiss, K.: Diacetyl emissions and airborne dust from butter flavorings used in microwave popcorn production, *J. Occup. Environ. Hyg.*, 3, 530–535, <https://doi.org/10.1080/15459620600909708>, 2006.
- Brasseur, G. P., Orlando, J. J., and Tyndall, G. S.: *Atmospheric Chemistry and Global Change*, Oxford University Press, New York, ISBN 9780195105216, 1999.
- Buzorius, G., Rannik, Ü., Mäkelä, J. M., Vesala, T., and Kulmala, M.: Vertical aerosol particle fluxes measured by eddy covariance technique using condensational particle counter, *J. Aerosol Sci.*, 29, 157–171, [https://doi.org/10.1016/S0021-8502\(97\)00458-8](https://doi.org/10.1016/S0021-8502(97)00458-8), 1998.
- Camredon, M., Aumont, B., Lee-Taylor, J., and Madronich, S.: The SOA/VOC/NO_x system: an explicit model of secondary organic aerosol formation, *Atmos. Chem. Phys.*, 7, 5599–5610, <https://doi.org/10.5194/acp-7-5599-2007>, 2007.
- Carnerero, C., Pérez, N., Reche, C., Ealo, M., Titos, G., Lee, H.-K., Eun, H.-R., Park, Y.-H., Dada, L., Paasonen, P., Kerminen, V.-M., Mantilla, E., Escudero, M., Gómez-Moreno, F. J., Alonso-Blanco, E., Coz, E., Saiz-Lopez, A., Temime-Roussel, B., Marchand, N., Beddows, D. C. S., Harrison, R. M., Petäjä, T., Kulmala, M., Ahn, K.-H., Alastuey, A., and Querol, X.: Vertical and horizontal distribution of regional new particle formation events in Madrid, *Atmos. Chem. Phys.*, 18, 16601–16618, <https://doi.org/10.5194/acp-18-16601-2018>, 2018.
- Casquero-Vera, J. A., Lyamani, H., Dada, L., Hakala, S., Paasonen, P., Román, R., Fraile, R., Petäjä, T., Olmo-Reyes, F. J., and Alados-Arboledas, L.: New particle formation at urban and high-altitude remote sites in the south-eastern Iberian Peninsula, *Atmos. Chem. Phys.*, 20, 14253–14271, <https://doi.org/10.5194/acp-20-14253-2020>, 2020.
- Chen, J., Jiang, S., Liu, Y. R., Huang, T., Wang, C. Y., Miao, S. K., Wang, Z. Q., Zhang, Y., and Huang, W.: Interaction of oxalic acid with dimethylamine and its atmospheric implications, *RSC Adv.*, 7, 6374–6388, <https://doi.org/10.1039/c6ra27945g>, 2017.
- Chen, J., Scircle, A., Black, O., Cizdziel, J. V., Watson, N., Wevill, D., and Zhou, Y.: On the use of multicopters for sampling and analysis of volatile organic compounds in the air by adsorption/thermal desorption GC-MS, *Air Qual. Atmos. Hlth.*, 11, 835–842, <https://doi.org/10.1007/s11869-018-0588-y>, 2018.
- Chen, T., Ge, Y., Liu, Y., and He, H.: N-nitration of secondary aliphatic amines in the particle phase, *Chemosphere*, 293, 133639, <https://doi.org/10.1016/j.chemosphere.2022.133639>, 2022.
- Correa, S. M., Arbilla, G., Marques, M. R. C., and Oliveira, K. M. P. G.: The impact of BTEX emissions from gas stations into the atmosphere, *Atmos. Pollut. Res.*, 3, 163–169, <https://doi.org/10.5094/APR.2012.016>, 2012.
- De Haan, D. O., Hawkins, L. N., Kononenko, J. A., Turley, J. J., Corrigan, A. L., Tolbert, M. A., and Jimenez, J. L.: Formation of nitrogen-containing oligomers by methylglyoxal and amines in simulated evaporating cloud droplets, *Environ. Sci. Technol.*, 45, 984–991, <https://doi.org/10.1021/es102933x>, 2011.
- Dehghani, M., Fazlzadeh, M., Sorooshian, A., Tabatabaee, H. R., Miri, M., Baghani, A. N., Delikhoon, M., Mahvi, A. H., and Rashidi, M.: Characteristics and health effects of BTEX in a hot spot for urban pollution, *Ecotox. Environ. Safe.*, 155, 133–143, <https://doi.org/10.1016/j.ecoenv.2018.02.065>, 2018.
- Dou, J., Lin, P., Kuang, B. Y., and Yu, J. Z.: Reactive oxygen species production mediated by humic-like substances in atmospheric aerosols: Enhancement effects by pyridine, imidazole, and their derivatives, *Environ. Sci. Technol.*, 49, 6457–6465, <https://doi.org/10.1021/es5059378>, 2015.
- Dumka, U. C., Moorthy, K. K., Kumar, R., Hegde, P., Sagar, R., Pant, P., Singh, N., and Babu, S. S.: Characteristics of aerosol black carbon mass concentration over a high altitude location in the Central Himalayas

- from multi-year measurements, *Atmos. Res.*, 96, 510–521, <https://doi.org/10.1016/j.atmosres.2009.12.010>, 2010.
- Dussault, P. and Sahli, A.: 2-Methoxy-2-propyl hydroperoxide: a convenient reagent for the synthesis of hydroperoxides and peracids, *J. Org. Chem.*, 57, 1009–1012, <https://doi.org/10.1021/jo00029a043>, 1992.
- Elomaa, T.: Mustan hiilen mittaus suodatinpohjaisilla sensoreilla, B.Sc. Thesis, University of Helsinki, 2022.
- Fermo, P., Artfñano, B., De Gennaro, G., Pantaleo, A. M., Parante, A., Battaglia, F., Colicino, E., Di Tanna, G., Goncalves da Silva Junior, A., Pereira, I. G., Garcia, G. S., Garcia Goncalves, L. M., Comite, V., and Miani, A.: Improving indoor air quality through an air purifier able to reduce aerosol particulate matter (PM) and volatile organic compounds (VOCs): Experimental results, *Environ. Res.*, 197, 1–8, <https://doi.org/10.1016/j.envres.2021.111131>, 2021.
- Fu, P., Kawamura, K., Usukura, K., and Miura, K.: Dicarboxylic acids, ketocarboxylic acids and glyoxal in the marine aerosols collected during a round-the-world cruise, *Mar. Chem.*, 148, 22–32, <https://doi.org/10.1016/j.marchem.2012.11.002>, 2013.
- Ge, X., Wexler, A. S., and Clegg, S. L.: Atmospheric amines – Part I. A review, *Atmos. Environ.*, 45, 524–546, <https://doi.org/10.1016/j.atmosenv.2010.10.012>, 2011.
- Hari, P. and Kulmala, M.: Station for Measuring Ecosystem-Atmosphere Relations (SMEAR II), *Boreal Environ. Res.*, 10, 315–322, 2005.
- Helin, A., Rönkkö, T., Parshintsev, J., Hartonen, K., Schilling, B., Lübbli, T., and Riekkola, M. L.: Solid phase microextraction Arrow for the sampling of volatile amines in wastewater and atmosphere, *J. Chromatogr. A*, 1426, 56–63, <https://doi.org/10.1016/j.chroma.2015.11.061>, 2015.
- Hemmilä, M.: Chemical Characterisation of Boreal Forest Air with Chromatographic Techniques, Doctoral thesis, University of Helsinki, Helsinki, ISBN 9789523361003, <http://urn.fi/URN:ISBN:978-952-336-100-3> (last access: 24 May 2023), 2020.
- Hemmilä, M., Hellén, H., Virkkula, A., Makkonen, U., Praplan, A. P., Kontkanen, J., Ahonen, L., Kulmala, M., and Hakola, H.: Amines in boreal forest air at SMEAR II station in Finland, *Atmos. Chem. Phys.*, 18, 6367–6380, <https://doi.org/10.5194/acp-18-6367-2018>, 2018.
- Hienola, A. I., Pietikäinen, J.-P., Jacob, D., Pozdun, R., Petäjä, T., Hyvärinen, A.-P., Sogacheva, L., Kerminen, V.-M., Kulmala, M., and Laaksonen, A.: Black carbon concentration and deposition estimations in Finland by the regional aerosol–climate model REMO-HAM, *Atmos. Chem. Phys.*, 13, 4033–4055, <https://doi.org/10.5194/acp-13-4033-2013>, 2013.
- Hoeben, W. F. L. M., Beckers, F. J. C. M., Pemen, A. J. M., Van Heesch, E. J. M., and Kling, W. L.: Oxidative degradation of toluene and limonene in air by pulsed corona technology, *J. Phys. D. Appl. Phys.*, 45, 055202, <https://doi.org/10.1088/0022-3727/45/5/055202>, 2012.
- Hyvärinen, A. P., Kolmonen, P., Kerminen, V. M., Virkkula, A., Leskinen, A., Komppula, M., Hatakka, J., Burkhardt, J., Stohl, A., Aalto, P., Kulmala, M., Lehtinen, K. E. J., Viisanen, Y., and Lihavainen, H.: Aerosol black carbon at five background measurement sites over Finland, a gateway to the Arctic, *Atmos. Environ.*, 45, 4042–4050, <https://doi.org/10.1016/j.atmosenv.2011.04.026>, 2011.
- Isidorov, V. A., Piroznikow, E., Spirina, V. L., Vasyanin, A. N., Kulakova, S. A., Abdulmanova, I. F., and Zaitsev, A. A.: Emission of volatile organic compounds by plants on the floor of boreal and mid-latitude forests, *J. Atmos. Chem.*, 79, 153–166, <https://doi.org/10.1007/s10874-022-09434-3>, 2022.
- Jacobson, M. Z.: Short-term effects of controlling fossil-fuel soot, biofuel soot and gases, and methane on climate, Arctic ice, and air pollution health, *J. Geophys. Res.-Atmos.*, 115, D14209, <https://doi.org/10.1029/2009JD013795>, 2010.
- Jang, M. and Kamens, R. M.: Atmospheric secondary aerosol formation by heterogeneous reactions of aldehydes in the presence of a sulfuric acid aerosol catalyst, *Environ. Sci. Technol.*, 35, 4758–4766, <https://doi.org/10.1021/es010790s>, 2001.
- Junninen, H., Lauri, A., Keronen, P., Aalto, P., Hiltunen, V., Hari, P., and Kulmala, M.: Smart-SMEAR: On-line data exploration and visualization tool for SMEAR stations, *Boreal Environ. Res.*, 14, 447–457, 2009.
- Kamens, R. M., Zhang, H., Chen, E. H., Zhou, Y., Parikh, H. M., Wilson, R. L., Galloway, K. E., and Rosen, E. P.: Secondary organic aerosol formation from toluene in an atmospheric hydrocarbon mixture: Water and particle seed effects, *Atmos. Environ.*, 45, 2324–2334, <https://doi.org/10.1016/j.atmosenv.2010.11.007>, 2011.
- Kanakidou, M., Seinfeld, J. H., Pandis, S. N., Barnes, I., Dentener, F. J., Facchini, M. C., Van Dingenen, R., Ervens, B., Nenes, A., Nielsen, C. J., Swietlicki, E., Putaud, J. P., Balkanski, Y., Fuzzi, S., Horth, J., Moortgat, G. K., Winterhalter, R., Myhre, C. E. L., Tsigaridis, K., Vignati, E., Stephanou, E. G., and Wilson, J.: Organic aerosol and global climate modelling: a review, *Atmos. Chem. Phys.*, 5, 1053–1123, <https://doi.org/10.5194/acp-5-1053-2005>, 2005.
- Kangasluoma, J. and Attoui, M.: Review of sub-3 nm condensation particle counters, calibrations, and cluster generation methods, *Aerosol Sci. Tech.*, 53, 1277–1310, <https://doi.org/10.1080/02786826.2019.1654084>, 2019.
- Karlberg, A.-T., Magnusson, K., and Nilsson, U.: Air oxidation of d-limonene (the citrus solvent) creates potent allergens, *Contact Dermatitis*, 26, 332–340, <https://doi.org/10.1111/j.1600-0536.1992.tb00129.x>, 1992.
- Kawamura, K. and Sakaguchi, F.: Molecular distributions of water soluble dicarboxylic acids in marine aerosols over the Pacific Ocean including tropics, *J. Geophys.-Res.*, 104, 3501–3509, 1999.
- Khare, P., Kumar, N., Kumari, K. M., and Srivastava, S. S.: Atmospheric formic acid and acetic acids: an overview, *Rev. Geophys.*, 37, 227–248, 1999.
- Kieloaho, A.-J.: Alkyl Amines in Boreal Forest and Urban Area, Doctoral thesis, University of Helsinki, ISBN 9789527091715, <http://urn.fi/URN:ISBN:978-952-7091-72-2> (last access: 24 May 2023), 2017.
- Kim, H., Park, Y., Kim, W., and Eun, H.: Vertical Aerosol Distribution and Flux Measurement in the Planetary Boundary Layer Using Drone, Particle and Aerosol Research, 14, 35–40, 2018.
- Kim, S. H., Kirakosyan, A., Choi, J., and Kim, J. H.: Detection of volatile organic compounds (VOCs), aliphatic amines, using highly fluorescent organic-inorganic hybrid perovskite nanoparticles, *Dyes Pigments*, 147, 1–5, <https://doi.org/10.1016/j.dyepig.2017.07.066>, 2017.

- Kim, S. J., Lee, J. Y., Choi, Y. S., Sung, J. M., and Jang, H. W.: Comparison of different types of SPME arrow sorbents to analyze volatile compounds in *cirsium setidens nakai*, *Foods*, 9, 785, <https://doi.org/10.3390/foods9060785>, 2020.
- Kivekäs, N., Sun, J., Zhan, M., Kerminen, V.-M., Hyvärinen, A., Komppula, M., Viisanen, Y., Hong, N., Zhang, Y., Kulmala, M., Zhang, X.-C., Deli-Geer, and Lihavainen, H.: Long term particle size distribution measurements at Mount Waliguan, a high-altitude site in inland China, *Atmos. Chem. Phys.*, 9, 5461–5474, <https://doi.org/10.5194/acp-9-5461-2009>, 2009.
- Kopperi, M., Ruiz-Jiménez, J., Hukkinen, J. I., and Riekkola, M. L.: New way to quantify multiple steroidal compounds in wastewater by comprehensive two-dimensional gas chromatography-time-of-flight mass spectrometry, *Anal. Chim. Acta*, 761, 217–226, <https://doi.org/10.1016/j.aca.2012.11.059>, 2013.
- Kristensen, K., Bilde, M., Aalto, P. P., Petäjä, T., and Glasius, M.: Denuder/filter sampling of organic acids and organosulfates at urban and boreal forest sites: Gas/particle distribution and possible sampling artifacts, *Atmos. Environ.*, 130, 36–53, <https://doi.org/10.1016/j.atmosenv.2015.10.046>, 2016.
- Krueve, A.: Influence of mobile phase, source parameters and source type on electrospray ionization efficiency in negative ion mode, *J. Mass Spectrom.*, 51, 596–601, <https://doi.org/10.1002/jms.3790>, 2016.
- Kulmala, M., Kontkanen, J., Junninen, H., Lehtipalo, K., Manninen, H. E., Nieminen, T., Petäjä, T., Sipilä, M., Schobesberger, S., Rantala, P., Franchin, A., Jokinen, T., Järvinen, E., Äijälä, M., Kangasluoma, J., Hakala, J., Aalto, P. P., Paasonen, P., Mikkilä, J., Vanhanen, J., Aalto, J., Hakola, H., Makkonen, U., Ruuskanen, T., Mauldin, R. L., Duplissy, J., Vehkamäki, H., Bäck, J., Kortelainen, A., Riipinen, I., Kurtén, T., Johnston, M. V., Smith, J. N., Ehn, M., Mentel, T. F., Lehtinen, K. E. J., Laaksonen, A., Kerminen, V. M., and Worsnop, D. R.: Direct observations of atmospheric aerosol nucleation, *Science*, 339, 943–946, <https://doi.org/10.1126/science.1227385>, 2013.
- Kulmala, M., Petäjä, T., Ehn, M., Thornton, J., Sipilä, M., Worsnop, D. R., and Kerminen, V. M.: Chemistry of atmospheric nucleation: On the recent advances on precursor characterization and atmospheric cluster composition in connection with atmospheric new particle formation, *Annu. Rev. Phys. Chem.*, 65, 21–37, <https://doi.org/10.1146/annurev-physchem-040412-110014>, 2014.
- Kumar, R., Barth, M. C., Nair, V. S., Pfister, G. G., Suresh Babu, S., Satheesh, S. K., Krishna Moorthy, K., Carmichael, G. R., Lu, Z., and Streets, D. G.: Sources of black carbon aerosols in South Asia and surrounding regions during the Integrated Campaign for Aerosols, Gases and Radiation Budget (ICARB), *Atmos. Chem. Phys.*, 15, 5415–5428, <https://doi.org/10.5194/acp-15-5415-2015>, 2015.
- Lan, H., Holopainen, J., Hartonen, K., Jussila, M., Ritala, M., and Riekkola, M. L.: Fully Automated Online Dynamic In-Tube Extraction for Continuous Sampling of Volatile Organic Compounds in Air, *Anal. Chem.*, 91, 8507–8515, <https://doi.org/10.1021/acs.analchem.9b01668>, 2019a.
- Lan, H., Zhang, W., Smått, J.-H., Koivula, R. T., Hartonen, K., and Riekkola, M.-L.: Selective extraction of aliphatic amines by functionalized mesoporous silica-coated solid phase microextraction Arrow, *Microchim. Acta*, 186, 412, <https://doi.org/10.1007/s00604-019-3523-5>, 2019b.
- Lan, H., Hartonen, K., and Riekkola, M. L.: Miniaturised air sampling techniques for analysis of volatile organic compounds in air, *TrAC-Trend. Anal. Chem.*, 126, 115873, <https://doi.org/10.1016/j.trac.2020.115873>, 2020.
- Lan, H., Ruiz-Jimenez, J., Leleev, Y., Demaria, G., Jussila, M., Hartonen, K., and Riekkola, M.-L.: Quantitative analysis and spatial and temporal distribution of volatile organic compounds in atmospheric air by utilizing drone with miniaturized samplers, *Chemosphere*, 282, 131024, <https://doi.org/10.1016/j.chemosphere.2021.131024>, 2021.
- Liu, Y., Monod, A., Tritscher, T., Praplan, A. P., DeCarlo, P. F., Temime-Roussel, B., Quivet, E., Marchand, N., Dommen, J., and Baltensperger, U.: Aqueous phase processing of secondary organic aerosol from isoprene photooxidation, *Atmos. Chem. Phys.*, 12, 5879–5895, <https://doi.org/10.5194/acp-12-5879-2012>, 2012.
- McGillen, M. R., Curchod, B. F. E., Chhantyal-Pun, R., Beames, J. M., Watson, N., Khan, M. A. H., McMahon, L., Shallcross, D. E., and Orr-Ewing, A. J.: Criegee Intermediate-Alcohol Reactions, A Potential Source of Functionalized Hydroperoxides in the Atmosphere, *ACS Earth Sp. Chem.*, 1, 664–672, <https://doi.org/10.1021/acsearthspacechem.7b00108>, 2017.
- McMurry, P. H.: The history of condensation nucleus counters, *Aerosol Sci. Technol.*, 33, 297–322, <https://doi.org/10.1080/02786820050121512>, 2000.
- Meena, G. S., Mukherjee, S., Buchunde, P., Safai, P. D., Singla, V., Aslam, M. Y., Sonbawne, S. M., Made, R., Anand, V., Dani, K. K., and Pandithurai, G.: Seasonal variability and source apportionment of black carbon over a rural high-altitude and an urban site in western India, *Atmos. Pollut. Res.*, 12, 32–45, <https://doi.org/10.1016/j.apr.2020.10.006>, 2021.
- Moorthy, K. K. and Babu, S. S.: Aerosol black carbon over Bay of Bengal observed from an island location, Port Blair: Temporal features and long-range transport, *J. Geophys. Res.-Atmos.*, 111, 1–10, <https://doi.org/10.1029/2005JD006855>, 2006.
- Ng, N. L., Kroll, J. H., Chan, A. W. H., Chhabra, P. S., Flagan, R. C., and Seinfeld, J. H.: Secondary organic aerosol formation from *m*-xylene, toluene, and benzene, *Atmos. Chem. Phys.*, 7, 3909–3922, <https://doi.org/10.5194/acp-7-3909-2007>, 2007.
- Nguyen, H. T. H., Takenaka, N., Bandow, H., Maeda, Y., De Oliva, S. T., Botelho, M. M. F., and Tavares, T. M.: Atmospheric alcohols and aldehydes concentrations measured in Osaka, Japan and in Sao Paulo, Brazil, *Atmos. Environ.*, 35, 3075–3083, [https://doi.org/10.1016/S1352-2310\(01\)00136-4](https://doi.org/10.1016/S1352-2310(01)00136-4), 2001.
- Oh, H. J., Ma, Y., and Kim, J.: Human inhalation exposure to aerosol and health effect: Aerosol monitoring and modelling regional deposited doses, *Int. J. Environ. Res. Pu.*, 17, 1–2, <https://doi.org/10.3390/ijerph17061923>, 2020.
- Olsen, R., Thorud, S., Hersson, M., Øvrebo, S., Lundanes, E., Greibrokk, T., Ellingsen, D. G., Thomassen, Y., and Molander, P.: Determination of the dialdehyde glyoxal in workroom air - Development of personal sampling methodology, *J. Environ. Monitor.*, 9, 687–694, <https://doi.org/10.1039/b700105n>, 2007.
- Pan, X. L., Kanaya, Y., Wang, Z. F., Liu, Y., Pochanart, P., Akiyama, H., Sun, Y. L., Dong, H. B., Li, J., Irie, H., and Takigawa, M.: Correlation of black carbon aerosol and carbon monoxide in the high-altitude environment of Mt. Huang in Eastern China, *Atmos. Chem. Phys.*, 11, 9735–9747, <https://doi.org/10.5194/acp-11-9735-2011>, 2011.

- Parshintsev, J., Ruiz-Jimenez, J., Petäjä, T., Hartonen, K., Kulmala, M., and Riekkola, M. L.: Comparison of quartz and Teflon filters for simultaneous collection of size-separated ultrafine aerosol particles and gas-phase zero samples, *Anal. Bioanal. Chem.*, 400, 3527–3535, <https://doi.org/10.1007/s00216-011-5041-0>, 2011.
- Parsons, G. E., Buckton, G., and Chatham, S. M.: The use of surface energy and polarity determinations to predict physical stability of non-polar, non-aqueous suspensions, *Int. J. Pharm.*, 83, 163–170, 1992.
- Peng, L., Li, Z., Zhang, G., Bi, X., Hu, W., Tang, M., Wang, X., Peng, P., and Sheng, G.: A review of measurement techniques for aerosol effective density, *Sci. Total Environ.*, 778, 146248, <https://doi.org/10.1016/j.scitotenv.2021.146248>, 2021.
- Perez, J. E., Kumar, M., Francisco, J. S., and Sinha, A.: Oxygenate-Induced Tuning of Aldehyde-Amine Reactivity and Its Atmospheric Implications, *J. Phys. Chem. A*, 121, 1022–1031, <https://doi.org/10.1021/acs.jpca.6b10845>, 2017.
- Petäjä, T., Rannik, Ü., Buzorius, G., Aalto, P., Vesala, T., and Kulmala, M.: Deposition Velocities of Ultrafine Particles Into Scots Pine Forest During Nucleation Events, *J. Aerosol Sci.*, 32, 143–144, [https://doi.org/10.1016/S0021-8502\(21\)00068-9](https://doi.org/10.1016/S0021-8502(21)00068-9), 2001.
- Petäjä, T., Laakso, L., Grönholm, T., Launiainen, S., Evelepeltoniemi, I., Virkkula, A., Leskinen, A., Backman, J., Manninen, H. E., Sipilä, M., Haapanala, S., Hämeri, K., Vanhala, E., Tuomi, T., Paatero, J., Aurela, M., Hakola, H., Makkonen, U., Hellén, H., Hillamo, R., Vira, J., Prank, M., Sofiev, M., Siitari-Kauppi, M., Laaksonen, A., Lehtinen, K. E. J., Kulmala, M., Visanen, Y., and Kerminen, V. M.: In-situ observations of Eyjafjallajökull ash particles by hot-air balloon, *Atmos. Environ.*, 48, 104–112, <https://doi.org/10.1016/j.atmosenv.2011.08.046>, 2012.
- Pusfitasari, E. D., Ruiz-Jimenez, J., Heiskanen, I., Jussila, M., Hartonen, K., and Riekkola, M.-L.: Aerial drone furnished with miniaturized versatile air sampling systems for selective collection of nitrogen containing compounds in boreal forest, *Sci. Total Environ.*, 808, 152011, <https://doi.org/10.1016/J.SCITOTENV.2021.152011>, 2022.
- Rajesh, T. A. and Ramachandran, S.: Black carbon aerosols over urban and high altitude remote regions: Characteristics and radiative implications, *Atmos. Environ.*, 194, 110–122, <https://doi.org/10.1016/j.atmosenv.2018.09.023>, 2018.
- Rinaldi, M., Decesari, S., Carbone, C., Finessi, E., Fuzzi, S., Ceburnis, D., O'Dowd, C. D., Sciare, J., Burrows, J. P., Vrekoussis, M., Ervens, B., Tsigaridis, K., and Facchini, M. C.: Evidence of a natural marine source of oxalic acid and a possible link to glyoxal, *J. Geophys. Res.-Atmos.*, 116, 1–12, <https://doi.org/10.1029/2011JD015659>, 2011.
- Rosado-Reyes, C. M. and Francisco, J. S.: Atmospheric oxidation pathways of acetic acid, *J. Phys. Chem. A*, 110, 4419–4433, <https://doi.org/10.1021/jp0567974>, 2006.
- Ruiz-Jimenez, J., Zanca, N., Lan, H., Jussila, M., Hartonen, K., and Riekkola, M. L.: Aerial drone as a carrier for miniaturized air sampling systems, *J. Chromatogr. A*, 1597, 202–208, <https://doi.org/10.1016/j.chroma.2019.04.009>, 2019.
- Safai, P. D., Kewat, S., Praveen, P. S., Rao, P. S. P., Momin, G. A., Ali, K., and Devara, P. C. S.: Seasonal variation of black carbon aerosols over a tropical urban city of Pune, India, *Atmos. Environ.*, 41, 2699–2709, <https://doi.org/10.1016/j.atmosenv.2006.11.044>, 2007.
- Sandeep, K., Panicker, A. S., Gautam, A. S., Beig, G., Gandhi, N., Sanjeev, S., Shankar, R., and Nainwal, H. C.: Black carbon over a high altitude Central Himalayan Glacier: Variability, transport, and radiative impacts, *Environ. Res.*, 204, 112017, <https://doi.org/10.1016/j.envres.2021.112017>, 2022.
- Sato, K., Ikemori, F., Ramasamy, S., Fushimi, A., Kumagai, K., Iijima, A., and Morino, Y.: Four- and five-carbon dicarboxylic acids present in secondary organic aerosol produced from anthropogenic and biogenic volatile organic compounds, *Atmosphere-Basel*, 12, 1703, <https://doi.org/10.3390/atmos12121703>, 2021.
- Sinclair, V. A., Ritvanen, J., Urbancic, G., Statnaia, I., Batrak, Y., Moisseev, D., and Kurppa, M.: Boundary-layer height and surface stability at Hyytiälä, Finland, in ERA5 and observations, *Atmos. Meas. Tech.*, 15, 3075–3103, <https://doi.org/10.5194/amt-15-3075-2022>, 2022.
- Takahama, S., Schwartz, R. E., Russell, L. M., Macdonald, A. M., Sharma, S., and Leaitch, W. R.: Organic functional groups in aerosol particles from burning and non-burning forest emissions at a high-elevation mountain site, *Atmos. Chem. Phys.*, 11, 6367–6386, <https://doi.org/10.5194/acp-11-6367-2011>, 2011.
- Teich, M., Schmidt pott, M., van Pinxteren, D., Chen, J., and Herrmann, H.: Separation and quantification of imidazoles in atmospheric particles using LC-Orbitrap-MS, *J. Sep. Sci.*, 43, 577–589, <https://doi.org/10.1002/jssc.201900689>, 2020.
- Tripathi, S. N., Srivastava, A. K., Dey, S., Satheesh, S. K., and Krishnamoorthy, K.: The vertical profile of atmospheric heating rate of black carbon aerosols at Kanpur in northern India, *Atmos. Environ.*, 41, 6909–6915, <https://doi.org/10.1016/j.atmosenv.2007.06.032>, 2007.
- Weingartner, E., Saathoff, H., Schnaiter, M., Streit, N., Bitnar, B., and Baltensperger, U.: Absorption of light by soot particles: Determination of the absorption coefficient by means of aethalometers, *J. Aerosol Sci.*, 34, 1445–1463, [https://doi.org/10.1016/S0021-8502\(03\)00359-8](https://doi.org/10.1016/S0021-8502(03)00359-8), 2003.
- Wen, L., Schaefer, T., He, L., Zhang, Y., Sun, X., Ventura, O. N., and Herrmann, H.: T- And pH-Dependent Kinetics of the Reactions of ·OH(aq) with Glutaric and Adipic Acid for Atmospheric Aqueous-Phase Chemistry, *ACS Earth Sp. Chem.*, 5, 1854–1864, <https://doi.org/10.1021/acsearthspchem.1c00163>, 2021.
- Yassaa, N., Brancaleoni, E., Frattoni, M., and Cicioli, P.: Isomeric analysis of BTEXs in the atmosphere using β -cyclodextrin capillary chromatography coupled with thermal desorption and mass spectrometry, *Chemosphere*, 63, 502–508, <https://doi.org/10.1016/j.chemosphere.2005.08.010>, 2006.
- Youn, J.-S., Crosbie, E., Maudlin, L. C., Wang, Z., and Sorooshian, A.: Dimethylamine as a major alkyl amine species in particles and cloud water: Observations in semi-arid and coastal regions, *Atmos. Environ.*, 122, 250–258, <https://doi.org/10.1016/j.atmosenv.2015.09.061>, 2015.
- Yu, K., Mitch, W. A., and Dai, N.: Nitrosamines and Nitramines in Amine-Based Carbon Dioxide Capture Systems: Fundamentals, Engineering Implications, and Knowledge Gaps, *Environ. Sci. Technol.*, 51, 11522–11536, <https://doi.org/10.1021/acs.est.7b02597>, 2017.
- Zahardis, J., Geddes, S., and Petrucci, G. A.: The ozonolysis of primary aliphatic amines in fine particles, *Atmos. Chem. Phys.*, 8, 1181–1194, <https://doi.org/10.5194/acp-8-1181-2008>, 2008.
- Zhang, R., Shen, J., Xie, H.-B., Chen, J., and Elm, J.: The role of organic acids in new particle formation from methanesulfonic

- acid and methylamine, *Atmos. Chem. Phys.*, 22, 2639–2650, <https://doi.org/10.5194/acp-22-2639-2022>, 2022.
- Zhang, Y., Wang, X., Wen, S., Herrmann, H., Yang, W., Huang, X., Zhang, Z., Huang, Z., He, Q., and George, C.: On-road vehicle emissions of glyoxal and methylglyoxal from tunnel tests in urban Guangzhou, China, *Atmos. Environ.*, 127, 55–60, <https://doi.org/10.1016/j.atmosenv.2015.12.017>, 2016.
- Zhao, Y. L., Garrison, S. L., Gonzalez, C., Thweatt, W. D., and Marquez, M.: N-nitrosation of amines by NO₂ and NO: A theoretical study, *J. Phys. Chem.-A*, 111, 2200–2205, <https://doi.org/10.1021/jp0677703>, 2007.
- Ziemann, P. J. and Atkinson, R.: Kinetics, products, and mechanisms of secondary organic aerosol formation, *Chem. Soc. Rev.*, 41, 6582–6605, <https://doi.org/10.1039/c2cs35122f>, 2012.